NASA SP-27

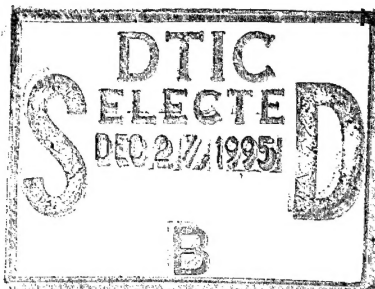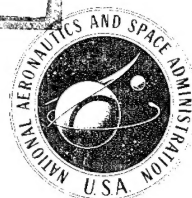# MATERIALS FOR

SPACE OPERATIONS

19951218 039

NATIONAL AERONAUTICS AND SPACE ADMINISTRATION ● Washington, D.C.

December 1962 ● Office of Scientific and Technical Information

*MSG DI4 DROLS PROCESSING-LAST INPUT IGNORED

--   ***DTIC DOES NOT HAVE THIS ITEM***
-- 1 - AD NUMBER: D429108
-- 5 - CORPORATE AUTHOR: NATIONAL AERONAUTICS AND SPACE ADMINISTRATION
--   WASHINGTON DC
-- 6 - UNCLASSIFIED TITLE: MATERIALS FOR SPACE OPERATIONS.
--11 - REPORT DATE: NOV 01, 1962
--12 - PAGINATION: 50P
--14 - REPORT NUMBER: NASA-SP-27
--20 - REPORT CLASSIFICATION: UNCLASSIFIED
--21 - SUPPLEMENTARY NOTE: 'MATERIALS FOR SPACE OPERATIONS', PAPERS
--   PRESENTED AT THE NSA-UNIVERSITY CONFERENCE ON THE SCIENCE AND
--   TECHNOLOGY OF SPACE EXPLORATION, 1-3 NOV 62, CHICAGO, IL. DEC 62.
--   (SEE PL-34391-PL-34395).
--22 - LIMITATIONS (ALPHA):   APPROVED FOR PUBLIC RELEASE: DISTRIBUTION
--   UNLIMITED. ~~AVAILABILITY: SUPERINTENDENT OF DOCUMENTS, GOVERNMENT~~
--   ~~PRINTING OFFICE, WASHINGTON, DC. $1.00 EACH.~~
--33 - LIMITATION CODES: 1 ▮

-- END   Y FOR NEXT ACCESSION   END

 Alt-Z FOR HELP3 ANSI   3 HDX 3   3 LOG CLOSED 3 PRINT OFF 3 PARITY

Foreword

The NASA-University Conference on the Science and Technology of Space Exploration, conducted in Chicago on November 1–3, 1962, was held "to provide an authoritative and up-to-date review of aeronautical and space science technology."

The scientific papers delivered at the conference were grouped for presentation by topics and are, in effect, 1962 state-of-the-art summaries. Accordingly, NASA has published under separate covers sixteen groups of conference papers to make them conveniently available to those interested in specific fields. This series (NASA SP–13 to NASA SP–28) is listed by title and price on the inside back cover.

All papers presented at the conference have also been published in a two-volume *Proceedings* (NASA SP–11) available from the Superintendent of Documents for $2.50 and $3.00, respectively. Those papers presented herein originally appeared on pages 439 to 484 of Volume 2 of NASA SP–11.

Contents

Space Environment and Its Effects on Materials

By Don D. Davis, Jr.

DON D. DAVIS, JR., *Assistant Head, High Temperature Materials Branch, Applied Materials and Physics Division, NASA Langley Research Center, received his Bachelor of Science degree in electrical engineering with distinction from the University of Nebraska in May 1944 and joined the Langley staff the following month in the Full-Scale Research Division. He earned his Master of Science degree in aeronautical engineering from the University of Virginia through Langley's graduate study program in June 1952.*

Davis directs research in ablation and transpiration cooling, kinetics of chemical oxidation, protective coatings for refractory materials, physics of meteoroid impact, satellite instrumentation for meteoroid detection, effect of space radiation on solar cells and on materials for such satellites as A-12 (Echo II), and shielding of spacecraft components from the effects of radiation. He will also direct a new 1.5-million-dollar space-vacuum laboratory that is now under construction at Langley to study the effects of the ultra-high vacuum of space on spacecraft materials and structural components. He pioneered the successful development of specialized transonic wind tunnels and directed loads research which resulted in rapid and substantial progress in understanding the factors that control aerodynamic loads at transonic speeds. His scholarly contribution of a complete and rational system for the design of acoustic filters has gained international recognition. Davis is Chairman of the local section of the Institute of the Aerospace Sciences, and is a member of the American Rocket Society, the Engineers' Club of the Virginia Peninsula, Sigma Tau and Pi Mu Epsilon honorary fraternities.

SUMMARY

Three aspects of the space environment that influence the selection of materials for use in spacecraft are considered: namely, vacuum, particle radiation, and meteoroids. To the best of our knowledge, vacuum effects have not so far been a serious problem for spacecraft. On the other hand, several spacecraft failures have been attributed to radiation, and confirmation of the suspected effects has been obtained in the laboratory. The extent of the hazard from meteoroids is uncertain. The most urgent need here is for reliable and accurate direct measurements of damage.

INTRODUCTION

This paper considers three aspects of the space environment which influence the selection of materials for use in spacecraft. These aspects are the scarcity of atoms (vacuum), the presence of charged particles (particle radiation), and the presence of interplanetary debris (meteoroids). In each case the most significant features of the environment will be mentioned, and then a few selected examples of the effect of this environment on engineering materials will be given.

SYMBOLS

d diameter of projectile
E energy
e electron (used in figs.)
P depth of penetration
p pressure in reference to vacuum effects
p proton in reference to radiation environment and
       effects (fig. 67–5)
T temperature

VACUUM

Space vehicles and their materials will be subjected to the vacuum environment for extended periods of time—months or even years. This environment is characterized by extremely low density, with a corresponding low pressure, and by a composition radically different from that at the earth's surface. Figure 67–1 shows the pressure as a function of altitude to 3,000 kilometers. (See ref. 1.) The width of the band indicates the variation in pressure from night to day. Pressure is used as the abscissa because there has been a tendency to define the space vacuum in terms of the pressure level. Actually, from the structural standpoint, the pressure forces in space are negligibly small. The physical phenomena of interest in connection with vacuum effects in space depend, instead, on the number of particles that come in contact with an exposed surface. Thus it is more meaningful to speak in terms of the number of particles in a unit volume rather than the pressure force exerted by those particles. Therefore, a scale has been added at the top of figure 67–1 to show the number density of the particles. At 3,000 kilometers there are one or two thousand particles per cubic centimeter, and farther outward from the earth it has been estimated that in interplanetary space there may be only about 10 particles per cubic centimeter. Thus the environment in which spacecraft components and materials must function contains only from perhaps ten to a few thousand particles per cubic centimeter.

In the few years since space exploration has become a reality, much effort has been directed toward simulation of the space vacuum environment in ground facilities. A few years ago the state of the art dictated number densities of about 10^9 particles per cubic centimeter (about 10^{-7} torr) in sizable vacuum chambers; today facilities are available to operate at number densities around 10^6 particles per cubic centimeter (about 10^{-10} torr). These facilities, however, still fall far short of the number densities in space of a few to a few thousand particles per cubic centimeter. Facility development is still progressing rapidly; therefore, it is possible that the space vacuum can be simulated in the future.

In the meantime, studies have been undertaken in currently available facilities to determine vacuum effects on spacecraft materials and components at the vacuum levels presently available. Many measurable effects have already been found, several of which would be detrimental to the accomplishment of a mission.

Perhaps the first problem area that comes to mind is material loss due to evaporation or sublimation into the space vacuum. Preliminary studies indicate that structural materials such as steel and aluminum alloys will not sublime at a rate so fast as to deteriorate significantly their load-carrying ability, even at moderate temperatures. (See ref. 2.) On the other hand, where the materials are applied as thin coatings, such as those used for thermal control, the sublimation is more serious. Figure 67–2 shows the effect of a vacuum environment on three thermal-control coatings that are intended for use on the
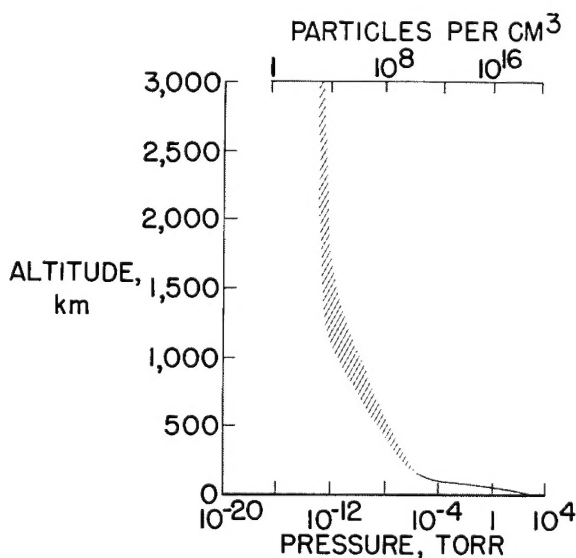

FIGURE 67–1.—Atmospheric pressure and number density of particles at altitudes to 3,000 km.
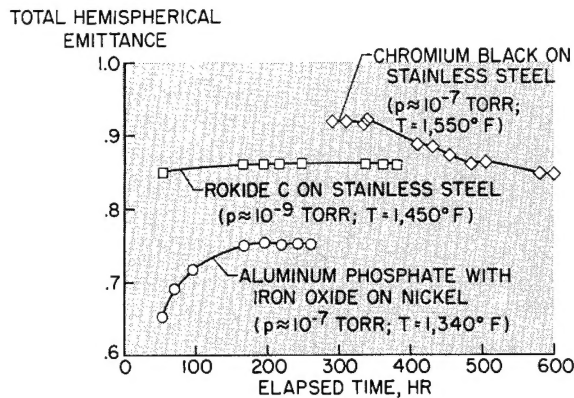
2

TOTAL HEMISPHERICAL
EMITTANCE

FIGURE 67-2.—Effects of exposure to vacuum on total hemispherical emittance at elevated temperatures for three coated materials intended for use as space radiators.

radiator of a space power plant. (See refs. 3 to 5.) The total hemispherical emittance is plotted as a function of the elapsed time in vacuum. The tests were conducted at elevated temperatures in the radiator operating range. The results show that the emittance can increase, can remain approximately the same, or can decrease because of exposure to vacuum. The cause of the observed changes in emittance has not yet been determined.

A second problem area arises because of the loss of adsorbed gas layers that are normally present on the surface of all materials. After prolonged exposure to the space-vacuum environment, a surface will lose all the surface adsorbed gases and will become "clean." As a result, it will behave differently when put in contact with another clean surface. Recent studies (ref. 6) have shown that cohesion or cold welding takes place. The studies were made by breaking a specimen in vacuum and then by placing the broken faces into contact again. The following table shows representative results from this study for 1018 steel.

Temperature, °C	Maximum cohesion, percent
500	96. 0
150	35. 9
25	18. 5

The primary variable is the temperature. The maximum cohesion shown in the column on the right is the percentage of the initial breaking force that was required to break the specimen the second time. These studies indicate that very significant cohesion, up to 96 percent, can take place under certain conditions. As the temperature is reduced, the cohesion is significantly reduced. The time that the broken faces were held apart was short enough in the last two cases to prevent significant contamination by the gas in the vacuum chamber; therefore, it is clear that the reduction in cohesion with decreasing temperature is not due to contamination. The occurrence of this cold-welding phenomenon could seriously affect the operation of spacecraft in the vacuum environment.

Studies of some mechanical properties of metals have indicated that the vacuum environment is not always detrimental. Creep-rupture and fatigue experiments indicate that under certain conditions metals are stronger in the nonreactive vacuum environment than in air at normal atmospheric pressure. (See ref. 7.) Figure 67-3 shows some fatigue data for type 316 stainless steel in vacuum and in air. The amplitude of the vibration is plotted against the number of cycles to failure. At a constant amplitude of vibration the material exhibited a substantially longer life in vacuum than in air. Data which indicate similar trends for creep rupture are also available. (See ref. 7.)
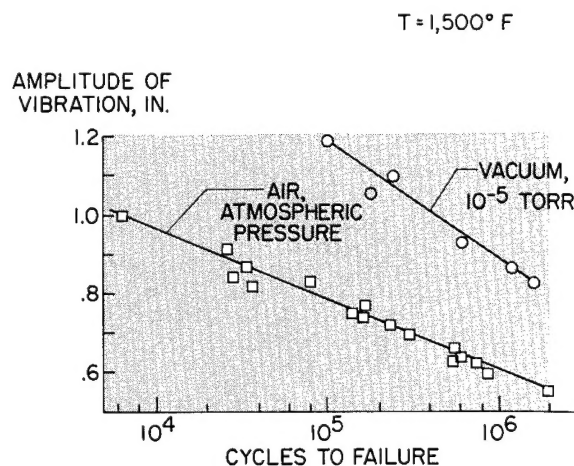
T = 1,500° F

AMPLITUDE OF
VIBRATION, IN.

FIGURE 67-3.—Effects of exposure to vacuum on fatigue life of type 316 stainless steel.

PARTICLE RADIATION

The particle radiation in space may be divided into several different categories as shown in figure 67–4. The primary galactic cosmic radiation (refs. 8 and 9) consists of positively charged particles of very high energy. The particles are primarily protons (85 percent) and alpha particles (13 percent), and the remainder consists of completely stripped nuclei with masses up to that of tin. As an overall average in free space, the flux is on the order of 2.5 particles/cm²-sec. Even with generous allowances for the high relative biological effectiveness of the heavy particles, the estimated dose delivered to an unprotected man in space would be on the order of only ½ rem (roentgen equivalent man) per week. Thus, even for man this radiation is of negligible effect, except on journeys of several years. For materials there should be essentially no effect from the galactic cosmic radiation, except perhaps on some photographic emulsions.

A second source of particle radiation in space is the solar cosmic radiation, or solar flare. (See refs. 8 to 12.) Solar flares originate in chromospheric disturbances of the sun, and their frequency is directly related to the period of the solar activity cycle. Low-energy events (with particles up to 400 Mev) and medium-energy events (with particles up to a few Bev) occurred with frequencies between 5 and 13 times a year in the period from 1935 to 1959. During the same period, high-energy events (with particles up to 20 Bev) occurred once or twice every 4 or 5 years.
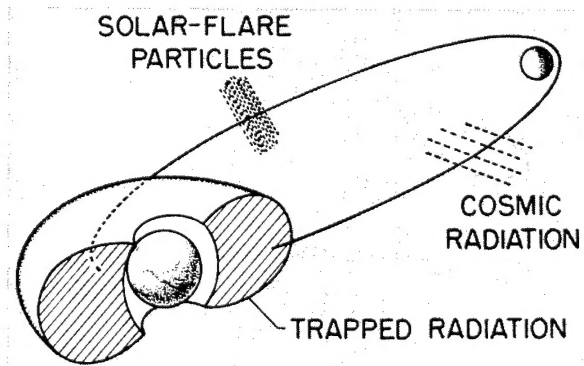
The primary danger in this case is to man because some of these flares can deliver large radiation doses. Basic research is being conducted at present along two lines: shielding studies, including studies of the secondary particles within the shield as well as preliminary work on systems of magnetic shielding, and studies leading toward the ability to predict solar flares a week or more in advance of their occurrence.

The presently available prediction criterion, when applied to a 3½-year period beginning in 1957 (ref. 11) would have allowed 117 four-day trips, only two of which would have encountered solar flares. During this same period, 77 seven-day trips would have been allowed with the unacceptably large number of 5 solar-flare encounters. A successful extension of prediction time to a period of 7 to 10 days would greatly relieve the shielding requirements for many lunar missions.

With regard to materials, the solar flare by itself may present problems for some of the more sensitive materials. Because of the sporadic nature of the solar flare, however, the time-averaged flux of particles will be relatively light. Thus, protection of materials from radiation damage due to flares may properly be considered as a subcase of protection from the natural trapped radiation near the earth.

The discovery and definition of this trapped radiation (refs. 8, 9, 13, and 14) shown schematically in figure 67–4 was one of our first scientific accomplishments with artificial satellites. The damaging potential of this radiation is such that the selection and protection of materials for satellites which will orbit for long periods of time in this region is our most pressing radiation damage problem.

Recent satellite measurements indicate that the older concept of two or more radiation belts is inadequate and misleading. A more appropriate concept is that the trapped radiation occupies one large and continuous region around the earth and that the intensity, energy, and type of radiation vary almost continuously throughout this region. The contours in figure 67–5 indicate the approximate spatial distribution of the trapped radiation. These contours are labeled with the counting rate that would

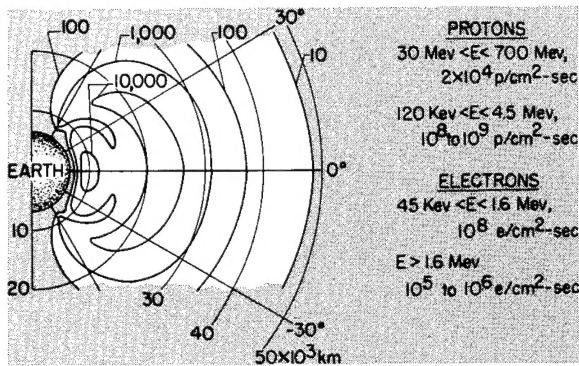FIGURE 67–4.—Schematic diagram of space radiation.

FIGURE 67–5.—Equal counting-rate contours of natural trapped radiation surrounding the earth.

be seen by a suitably shielded Geiger-tube and are useful only as a qualitative indication of those portions of the region which pose the most severe radiation problems.

Since the particles are trapped in the magnetic field of the earth, the intensities are highest near the equatorial plane and are substantially lower near the polar regions. The minimum altitude for significant counting rates varies around the earth because the magnetic and geometric axes of the earth are substantially offset from each other. Over the South Atlantic, counting rates begin to increase at an altitude of about 400 kilometers, whereas on the opposite side of the earth the corresponding altitude is about 1,300 kilometers. Thus it is possible, when allowed by the mission requirements, to orbit below this radiation. Estimates of the outermost extent of the trapped radiation range as high as 10 earth radii.

The maximum fluxes of the particles are shown at the right in figure 67–5. The high-energy protons are the most spectacular portion of the flux and are largely confined to the small inner high-flux contour. The maximum flux between 30 Mev and 700 Mev is on the order of 2×10^4 protons/cm²-sec. Low-energy protons are found almost throughout the entire region. The measured fluxes between 120 Kev and 4.5 Mev range on the order of 10^8 to 10^9 protons/cm²-sec. There is also a substantial flux of low- and medium-energy electrons (45 Kev to 1.6 Mev) on the order of 10^8 electrons/cm²-sec throughout most of the region shown. The higher energy electrons are largely confined

to the outer high-flux contour with fluxes on the order of 10^5 to 10^6 electrons/cm²-sec.

More recently, an additional component of space radiation has been added by the high-altitude nuclear explosion of July 9, 1962. (See ref. 15.) This explosion created a new belt of electron radiation around the earth. The new belt is shown schematically in figure 67–6. It is somewhat smaller in extent and lower than the natural belt. Large fluxes are observed at only 200 kilometers above the earth over the South Atlantic; on the opposite side of the earth the minimum altitude is about 650 kilometers. These low altitudes are significant since it is at present almost impossible to escape radiation exposure by means of low-altitude orbits. Although the flux decay rate in the heart of the new belt seems negligibly small, some decay has been observed at the lowest altitudes. This decay will eventually ease the problem; however, it will be several years before radiation resistance can again be neglected for orbits sufficiently high to achieve long lifetimes. The new belt extends out to about 25,000 kilometers from the center of the earth. Maximum fluxes on the order of 10^9 electrons/cm²-sec have been observed. In contrast to the natural radiation, where over 99 percent of the electrons occur with energies of less than 1.6 Mev, the electrons of the new belt seem to occur with a typical fission energy spectrum. A breakdown of this spectrum by energy is given in the table on the right of the figure.

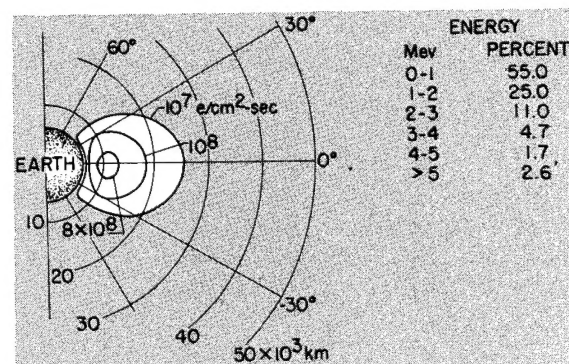The large flux and higher energy of the electrons in the new belt means that adequate

FIGURE 67–6.—Equal flux contours of new artificial electron belt.

5

heavy shielding must be provided for many radiation-sensitive devices. In many cases this shielding will be very heavy, and it will be needed where either no shielding or only minimal shielding was previously required. The need is best illustrated by the fact that, of those satellites in orbit at the time of the blast, three were inactiviated by radiation damage to their solar cells within about a month; indeed, one failed in only three days.

Even before the new belt was formed, it was evident that space radiation possessed a severe damaging potential insofar as materials such as semiconductors and plastics are concerned. (The new belt has only increased the urgency of the need for data in these areas.) Consequently, the NASA has installed or is preparing to install a number of accelerators ranging from 1.0-Mev electron accelerators to a 600-Mev proton synchrocyclotron in order to study the problem. In addition, a substantial amount of contract research with private industry, universities, and other government organizations is already under way. Three examples have been selected for discussion in this paper. These examples are intended only to illustrate some of the work already in progress; the interests of the NASA in this area are far broader than these examples alone might indicate.

The first example concerns transistors. The sensitivity of many solid-state devices to radiation has led to a major program in which a number of available accelerators have been utilized to study the effect of proton irradiation on transistors. (See ref. 16.) Energies from 22 Mev to 440 Mev have been utilized to date. The data shown in figure 67–7 are typical and

FIGURE 67–7.—Effect of exposure to 40-Mev protons on current gain of two transistors.

were obtained by using the 40-Mev linear proton accelerator at the University of Minnesota. Here the small-signal current gain, or essentially, the transistor's ability to operate as an amplifier, is plotted against the total dose in protons per square centimeter. The scale at the top shows the approximate time equivalent in terms of years in orbit in the worst part of the radiation belt. The two broad bands show the degradation of two different NPN silicon transistors, the 2N743 and the 2N337. The width of the bands indicates the scatter among the data for approxiately a half-dozen samples of each type. The dramatic decrease in current gain for the 2N337 is typical of the lower frequency transistors tested; the negligible degradation of the 2N743 is typical of the highest frequency transistors tested. The lesser degradation of the higher frequency units is consistent in other types of construction. Indeed, the increased radiation resistance of the higher frequency units led to one of the design choices that was made in the case of the Telstar satellite.

The solar cell is an example of a solid-state device that is extremely sensitive to radiation (refs. 16 and 17) and at the same time difficult to shield from radiation when operating in space. Substantial additional interest in the solar-cell problem has been engendered by the aforementioned recent loss of three satellites to the new artificial radiation belt because of solar-cell damage. Figure 67–8 shows the spectral variation of short-circuit current for a P on N silicon solar cell before and after electron irradiation. The energy of the electrons was 0.65 Mev. The total dose is approximately that which might be encountered in a year in a practical orbit within the new belt. Immediately evident is the large loss of output in the infrared region where the output of the undamaged cell was highest. On the other hand, there is little or no degradation at the shorter wavelengths. The long wavelengths penetrate deeply in the cell, whereas the short wavelengths are absorbed at or near the surface. Thus the changes shown in figure 67–8 indicate that most of the damage is done in the base material well below the actual junction, which is about 1 micron deep.
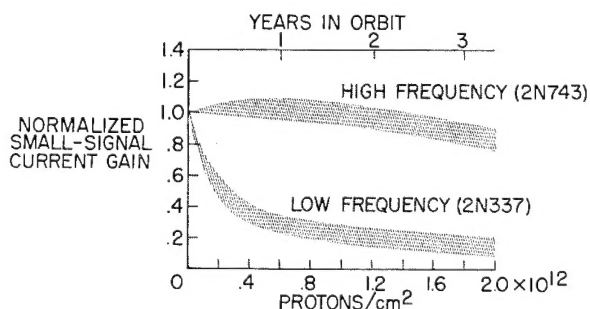
.65 Mev; 2.59 ×10^{15} e/cm^2;
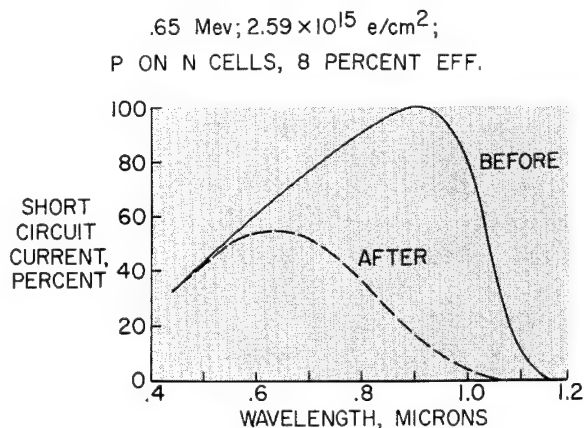P ON N CELLS, 8 PERCENT EFF.

FIGURE 67–8.—Effect of exposure to 0.65-Mev electrons on spectral variation of short-circuit current for a P on N silicon solar cell.

One approach to improved radiation resistance in a solar cell is obvious from figure 67–8, that is, to improve the response in the short-wavelength region where the radiation has little effect. This is precisely what is done in the so-called blue-sensitive shallow-diffused cells which are indeed more radiation resistant. Far greater improvements are to be had in the use of N on P cells rather than the P on N cells shown here. (See ref. 17.) The radiation resistance of the N on P cells is so intrinsically superior that these cells are the presently preferred type and their use is indicated whenever permitted by the presently small but rapidly increasing production rate.

The NASA is currently sponsoring a substantial amount of research in industry, not only on silicon solar cells, but also on newer cells such as gallium arsenide, and even on vapor-deposited cells which could be deposited directly over large areas of a space vehicle.

Another approach to radiation resistance is to shield the item of concern with a thickness of some material which is adequate to stop all or most of the particles incident upon the item. In the case of solar cells and other light-sensitive or optical systems, this shield must not only be transparent, but it must also remain transparent under radiation. Most glasses do color under radiation. (See refs. 18 and 19.) The mechanism in most cases is described as the combination of displaced electrons with negative-ion sites (or vacancies) to form color centers. Such coloration may mean that the

shield, by stopping a major portion of the light, does more harm in some cases than the radiation would have done if no shielding had been provided.

Recently, this phenomenon has been studied at the Langley Research Center of the NASA in connection with providing shielding for the solar cells of a specific orbital spacecraft. This spacecraft will orbit well within the artificial belt and the major hazard will be from high-energy electrons. Many glasses were irradiated with 1.2-Mev electrons in this program. The results for three quartzes are shown in figure 67–9. Here the relative transmission of the glass, averaged over the solar-cell response spectrum, is plotted as a function of the total dose in electrons per square centimeter. The end point corresponds to one year in orbit for the particular payload. Results are shown for three different quartz samples, two fused and one vapor deposited. The vapor-deposited sample shows essentially no decrease in transmission. Of the two fused samples, one shows about a 10-percent loss and the other, about a 40-percent loss in transmission after a year's time. In the worst case, most of the coloration came very early, so that the solar-cell output behind this shield would have been reduced to a critical level within a very few weeks.

The actual differences in the materials shown here are presently believed to be related to the degree of impurity. The poorest quartz had 50 to 70 parts per million of impurities; the best had less than 1 part per million. The practical conclusion to be drawn from these results is that extreme care is essential in the selection of transparent radiation shielding and that
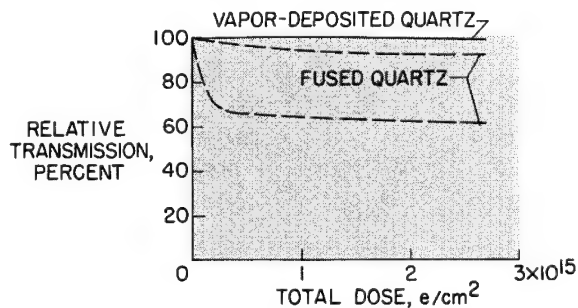

FIGURE 67–9.—Effect of exposure to 1.2-Mev electrons on solar-energy transmission for three types of quartz windows.

this care should extend to the point of actually exposing samples to radiation as a quality control check.

METEOROIDS

The discussion will turn now to the meteoritic debris in space. Damage to spacecraft that would result in danger to the occupants or that would prevent the fulfillment of the mission must not be allowed to occur. This is a difficult problem for the space-vehicle designer, because at the present time there is a large uncertainty with regard to the size and weight of meteoroids that will be encountered and with regard to the damage that they will do. The examination of the status of this particular problem will begin with a review of our knowledge of the space environment.

The available information on the meteoroid environment in space is illustrated in figure 67–10 (adapted from ref. 20). The cumulative influx rate in particles per square meter per second is plotted as a function of the particle mass in grams. The cumulative influx rate corresponding to a mass x is the total number of particles of mass x, or less, that pass through one square meter in one second. Logarithmic scales are used on both axes. The solid lines at the lower right show estimates of the meteoroid environment that are derived from astronomical observations of meteors in the earth's atmosphere. The observable quantities are the influx rate and the light intensity. By making

certain assumptions, it is possible to derive a relationship between the light intensity and the particle mass. With this relationship in hand it is possible to plot the astronomical observations in the form that they are shown in this figure. There is a very large difference between the two solid lines that are shown. This difference stems from a difference in the estimates of the astronomers for the relationship between the light intensity and the particle mass. At a cumulative influx rate of 10^{-12} particles per square meter per second, a particle mass of about 10^{-2} grams is indicated by the lower curve and a mass of about 2 grams by the upper curve. These estimates of the mass differ by a factor of 200 to 1, and thereby produce an extremely large uncertainty in the flux-mass relationship. The particles of most interest with regard to spacecraft damage are smaller than the observed meteors. Estimates of the flux of these particles have been obtained by straight-line extrapolation from the observed data. These extrapolations are shown by the dashed lines extending to the left from the solid lines that were derived from meteor observations. At the other end of the scale there are data points representing actual flight measurements of micrometeoroid impact rates. Most of these measurements were obtained by using a microphone type of dust-particle sensor; the slope of the line faired through these points is considerably greater than the slope of the lines that were derived from astronomical observations. The range of most interest to the spacecraft designer lies between the small particles observed in the dust measurements and the meteors observed from the ground. In this range there is at the present time much uncertainty both with regard to the level of the distribution curve and with regard to the slope of this curve.

The data and estimates shown in this figure apply in the immediate vicinity of the earth. The meteoroid hazard in other regions of space is also of concern to the NASA. In the Apollo program, for example, the meteoroid hazard in the vicinity of the moon and on the surface of the moon must be considered. In an attempt to get a feel for this problem in the absence of actual measurements, Gault, Shoemaker, and Moore have recently studied the problem of
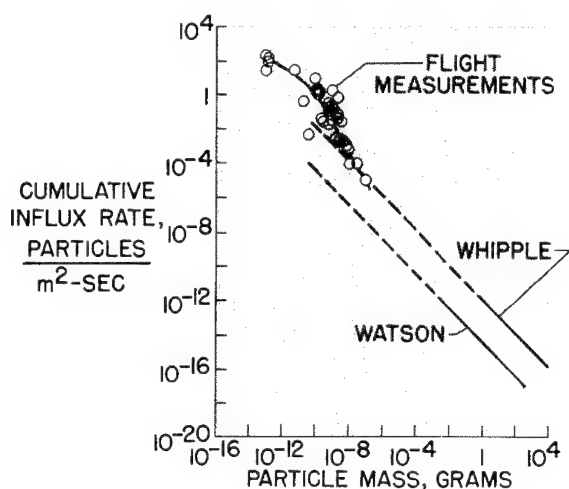

FIGURE 67–10.—Cumulative influx rate of meteoroids in vicinity of earth as a function of mass.

hypervelocity impact of a projectile on a basalt-rock surface. The results of their analysis (which are unpublished) suggest a heavy flux of debris in the vicinity of the moon due to meteoroid collisions with the moon, but they do not provide numerical values for use in spacecraft design. If there is, in fact, a heavy concentration of particles in the mass range that might be expected to puncture spacecraft, it would, of course, constitute a serious problem in the Apollo program.

In addition to the uncertainty as to the mass of the particles that will be encountered, there is a further uncertainty as to the damage that will be caused by a particle of known mass and velocity. This is illustrated in figure 67–11, which presents plots of penetration as a function of velocity as estimated by three of the many formulas that have been proposed. The symbols P and d are defined by the sketch at the right. The curves labeled Huth et al. and Charters and Summers are based on experimental data obtained at velocities well below those that are typical of meteoroids. (See refs. 21 and 22.) Bjork's curve is strictly theoretical. (See refs. 23 and 24.) At a velocity of 30,000 to 40,000 kilometers per second, which is typical of meteoroids, the penetration appears to be uncertain by a factor of about 10. There is a pressing need for the development of an adequate penetration theory.

The combined effect of the two uncertainties that have been discussed is such that, at the present time, if a spacecraft designer is faced with the problem of insuring that the number of penetrations does not exceed a given value, he is faced with an uncertainty of about 20 to 1 in the thickness of material that he must use.

A considerable amount of effort has been devoted to systems designed to protect a spacecraft from penetration by meteoroids. One of the most promising devices is the meteoroid bumper, which is simply a thin sheet of material that is placed outside and at a distance from the structural wall of a spacecraft with the object of providing protection from damage by meteoroids. Figure 67–12 is a sequence of photographs that show the mechanism by which a meteoroid bumper provides protection. (See ref. 24.) In the first photograph, the vertical dark line at the left is a thin plate which has been impacted by a spherical projectile coming from the left. The projectile is in the dark area to the right of the plate. Some of the material from the plate can be seen flying back to the left. The two vertical lines to the right of the projectile are not in its path. They are simply markers which have been used to provide a length reference in the photographs. The first photograph was taken 6.5 microseconds after the initial impact. In the next photograph, at 9.8 microseconds, some light is visible through the debris at the right of the plate. The projectile has been broken into many small fragments in passing through the plate and the rest of the photographs show that these fragments disperse as they travel away from the plate. The impact of these many small particles dispersed over a wide area, of course, produces a great deal less damage than would the original projectile. Reference 25 also presents information on the influence of the geometrical arrangement on the effectiveness of bumpers.

CONCLUDING REMARKS

A brief account of the state of our knowledge of the effects of the space environment on engineering materials will be attempted in conclusion. With regard to vacuum, a few problems have turned up in the laboratory, but the effects of the extreme vacuum of space are largely unexplored and therefore unknown. To the best of our knowledge (and in this area
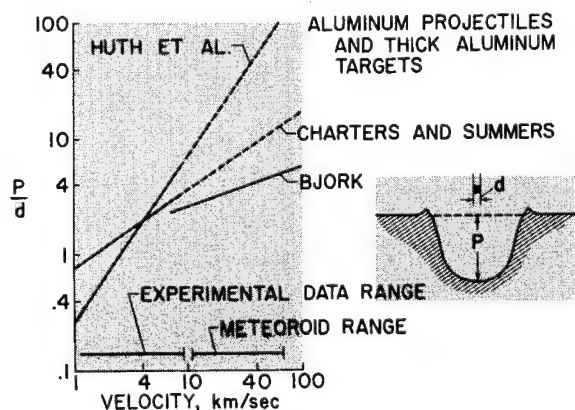
FIGURE 67–11.—Three estimates of penetration depth as a function of velocity for high-velocity aluminum projectiles impacting thick aluminum targets.

TIME ELAPSED SINCE IMPACT

6.5 μ SEC   9.8 μ SEC   13.1 μ SEC

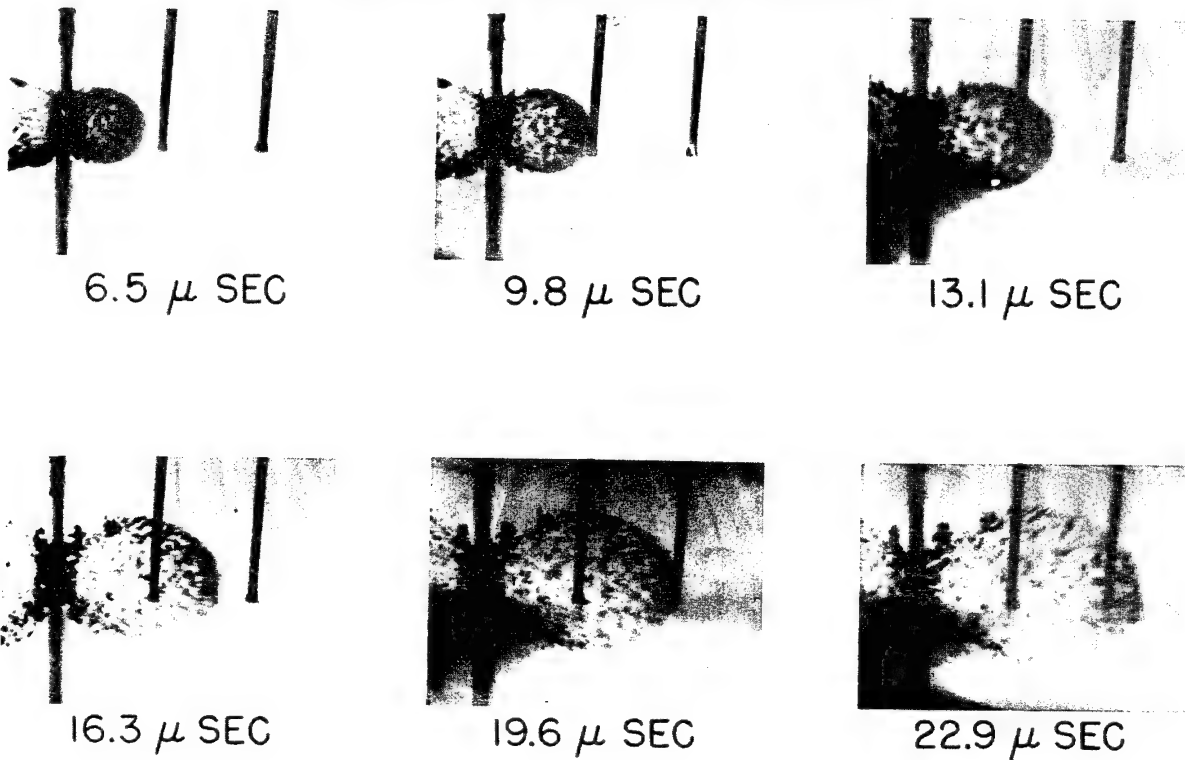16.3 μ SEC   19.6 μ SEC   22.9 μ SEC

FIGURE 67–12.—Sequence of photographs showing breakup and dispersion of a high-velocity projectile by a meteoroid bumper.

the best is not good), vacuum effects have not so far been a serious problem for spacecraft.

The situation with regard to radiation is entirely different. Several spacecraft failures have been attributed to radiation, and confirmation of the suspected effects has been obtained in the laboratory. Because these effects have been so detrimental, it is obvious that there will be a great demand upon the operators of charged particle accelerators to produce engineering results and to evaluate engineering developments in this area.

With regard to the meteoroid environment, the status is clear, but the hazard is not. In other words, it is perfectly obvious that the extent of the hazard is not known—not even within an order of magnitude. The most urgent need here is for some reliable and accurate direct measurements of damage that can be used as a check on the work of both the theoreticians and the design engineers. Rapid progress would follow the establishment of even a single point of this nature in which real confidence could be placed.

REFERENCES

1. JASTROW, R., and KYLE, H.: The Earth Atmosphere. Sec. 2.1 of Handbook of Astronautical Engineering, First ed., Heinz Hermann Koelle, ed., McGraw-Hill Book Co., Inc., 1961, pp. 2–2—2–13.
2. JAFFE, LEONARD D., and RITTENHOUSE, JOHN B.: Behavior of Materials in Space Environments. ARS Jour., vol. 32, no. 3, Mar. 1962, pp. 320–346.
3. ANON.: Measurement of Spectral and Total Emittance of Materials and Surfaces Under Simulated Space Conditions. Rep. No. PWA–1863 (Contract No. NASW–104), Pratt & Whitney Aircraft, 1960.

4. ANON.: Progress Report on the Determination of the Emissivity of Materials During the Period From July 1, 1960, Through September 30, 1960. Rep. No. PWA–1877 (Contract NASW–104), Pratt & Whitney Aircraft, 1960.

5. ASKWYTH, WILLIAM H.: Progress Report—Determination of the Emissivity of Materials. Rep. No. PWA–2043 (Contract NASw–104), Pratt & Whitney Aircraft, 1961.

6. HAM, JOHN L.: Investigation of Adhesion and Cohesion of Metals in Ultrahigh Vacuum. NRC Proj. No. 42–1–0121 (Contract No. NASr–48), Nat. Res. Corp. (Cambridge, Mass.), Dec. 15, 1961–Mar. 15, 1962.

7. ACHTER, M. R.: Effects of High Vacuum on Mechanical Properties. First Symposium—Surface Effects on Spacecraft Materials, Francis J. Clauss, ed., John Wiley & Sons, Inc., c.1960, pp. 286–306.

8. FOELSCHE, TRUTZ: Current Estimates of Radiation Doses in Space. NASA TN D–1267, 1962.

9. VOSTEEN, LOUIS F.: Environmental Problems of Space Flight Structures. I. Ionizing Radiation in Space and Its Influence on Spacecraft Design. NASA TN D–1474, 1962.

10. ANDERSON, KINSEY A., and FICHTEL, CARL E.: Discussions of Solar Proton Events and Manned Space Flight. NASA TN D–671, 1961.

11. ANDERSON, KINSEY A.: Preliminary Study of Prediction Aspects of Solar Cosmic Ray Events. NASA TN D–700, 1961.

12. OGILVIE, KEITH W.: Solar Protons. NASA TN D–1139, 1962.

13. VAN ALLEN, J. A.: The Earth and Near Space. Bull. Atomic Scientists, vol. XVII, no. 5–6, May–June 1961, pp. 218–222.

14. KOLCUM, EDWARD H.: Research Challenge Encompasses Galaxy. Aviation Week and Space Technology, vol. 77, no. 15, Oct. 8, 1962, pp. 54–67.

15. HESS, W. N., and NAKADA, PAUL: Artificial Radiation Belt Discussed in Symposium at Goddard Space Center. Science, vol. 138, no. 3536, Oct. 5, 1962, pp. 53–54.

16. HULTEN, W. C., HONAKER, W. C., and PATTERSON, JOHN L.: Irradiation Effects of 22 and 240 Mev Protons on Several Transistors and Solar Cells. NASA TN D–718, 1961.

17. AUKERMAN, L. W.: Proton and Electron Damage to Solar Cells. REIC Rep. No. 23 (Contract No. AF 33(616)–7375), Battelle Memorial Inst., Apr. 1, 1962.

18. RILEY, W. C., COPPINS, W. G., and DUCKWORTH, W. H.: The Effect of Nuclear Radiation on Glass. REIC Tech. Memo. 9 (Contract No. AF 33(616)–5171), Battelle Memorial Inst., Nov. 30, 1958.

19. LEVY, PAUL W.: Radiation Effects in Glass and Other Materials. Physics Today, vol. 15, no. 9, Sept. 1962, pp. 19–23.

20. ALEXANDER, W. M., McCRACKEN, C. W., SECRETAN, L., and BERG, O. E.: Review of Direct Measurements of Interplanetary Dust From Satellites and Probes. X–613–62–25, Goddard Space Flight Center, NASA, 1962.

21. HUTH, J. H., THOMPSON, J. S., and VAN VALKENBURG, M. E.: Some New Data on High-Speed Impact Phenomena. Jour. Appl. Mech., vol. 24, no. 1, Mar. 1957, pp. 65–68.

22. SUMMERS, JAMES L.: Investigation of High-Speed Impact: Regions of Impact and Impact at Oblique Angles. NASA TN D–94, 1959.

23. BJORK, R. L.: Numerical Solutions of the Axially Symmetric Hypervelocity Impact Process Involving Iron. U.S. Air Force Project RAND S–103 (ASTIA Doc. No. AD 305657), The RAND Corp., Dec. 16, 1958.

24. BJORK, R. L.: Meteoids Versus Space Vehicles. ARS Jour., vol. 31, no. 6, June 1961, pp. 803–807.

25. HUMES, DON, HOPKO, R. N., and KINARD, WILLIAM H.: An Experimental Investigation of Single Aluminum "Meteor Bumpers." Proc. of the Fifth Symposium on Hypervelocity Impact (Denver), vol. 1, pt. 2, Apr. 1962, pp. 567–580. (Sponsored by U.S. Navy, U.S. Army, and U.S. Air Force.)

Nonmetallic Materials for Spacecraft

By George F. Pezdirtz

DR. GEORGE F. PEZDIRTZ, *Head, Spacecraft Materials Section, Applied Materials and Physics Division, NASA Langley Research Center, received his Bachelor of Science degree in Chemistry and his Doctorate in Organic Chemistry from the University of Notre Dame in 1955 and 1960, respectively. The W. W. Barton Research Fellowship was awarded to him in 1956 by the University. His thesis was on "The Effects of High Energy Electrons on a Series of Saturated Polyesters." During 1955 and 1956, he was a chemistry laboratory instructor at Notre Dame. He was a special lecturer in physics and chemistry for Indiana University Extension (South Bend) in 1956–1957. Dr. Pezdirtz carried out basic research on heterogeneous polymerization catalysts for polyolefins at the Texaco Research Center, Beacon, New York during 1958–1960. Dr. Pezdirtz, who joined the Langley staff in November 1960 as an Aero-Space Technologist, has specialized in radiation chemistry of polymers, heterogenous polymerization catalysts, and thermal control surfaces. He is responsible for the ultrathin inorganic coating for thermal control of the 135-foot-diameter A-12 (Echo II) passive communications balloon scheduled to be launched into orbit next year. Dr. Pezdirtz has 15 patent applications on heterogeneous polymerization catalysts for Texaco research; he is author of several NASA publications and has presented papers before technical societies on erectable space structures. He is a member of the American Chemical Society, Research Society of America, and American Association for Advancement of Science.*

SUMMARY

Nonmetallic materials have many unusual and desirable properties for use in spacecraft applications, but their sensitivities to the ultraviolet and high-energy ionizing radiation of space have created problems— some as yet unsolved. The problems of thermal control coatings, polymers, and composites in space applications are discussed. The need for new nonmetallic materials with unusual properties such as inorganic polymers is also examined.

INTRODUCTION

The unusual and highly advantageous properties of polymers have made these materials very desirable for use in aerospace programs. Polymers, which include plastics, rubbers, and most adhesives, have yielded significant reduc-

tions in the overall cost of aerospace systems. This reduction in cost may be expressed in terms of money, energy, weight, or time. It is the purpose of this paper to review some of the properties of polymers which are responsible for these savings and which have further resulted in many unique applications.

In aerospace projects, one of the ever-increasing needs is for materials with high strength-to-weight ratios, good temperature properties, availability, and ease of fabrication. Although the development of polymeric and other nonmetallic materials is not yet commensurate with the need, these materials have such fundamental advantages that they have already made substantial contributions to the space program.

SYMBOLS

p pressure
T temperature
t thickness
α_s absorptance of solar radiation
ϵ emittance of solar radiation
ϵ_λ emittance as a function of wave length
λ wave length

SOME RELATIVE PROPERTIES OF POLYMERS AND METALS

Some of the relative physical properties of metals and polymers are shown in figure 68–1.
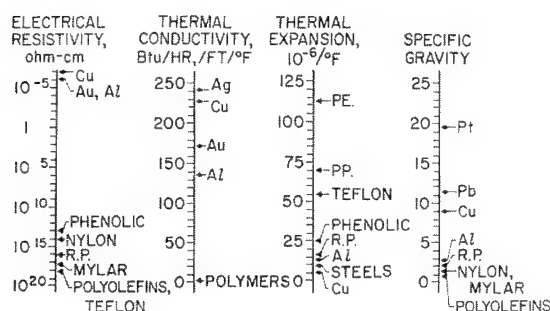
FIGURE 68–1.—Relative physical properties of metals and nonmetals. R.P. denotes reinforced plastics; PE., polyethylenes; PP., polypropylenes.

(See ref. 1.) One of the greatest differences in the properties of these two classes of materials is the electrical resistivity: metals are at the low end of the scale, and polymers are at the high end. Concurrent with the low electrical conductivity of polymers is low thermal conductivity. The higher coefficient of thermal expansion for polymers is another variable which can obviously lead to problems when the two materials are joined in composite form; however, in some instances, the lower modulus of elasticity and higher permissible strain of the polymers can alleviate this difference.

Some of the relative mechanical properties of metals and polymers are illustrated in figure 68–2. In general, polymers have a lower spectrum of tensile strength and a lower modulus of elasticity than metals, although it should be noted that the epoxy-glass composite does have a relatively high modulus of elasticity and one of the highest strength-to-weight ratios of the structural materials. The service temperature of polymers is also considerably lower than that
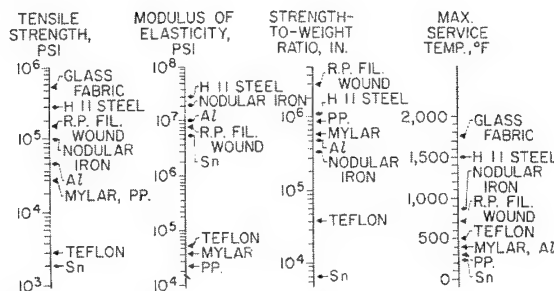
FIGURE 68–2.—Relative mechanical properties of metals and nonmetals. PP. denotes polypropylenes; R.P., reinforced plastics.

of metals, primarily as a result of the weaker organic carbon-to-carbon bonds in contrast to the strong metallic bonds of the metals and alloys. At present this low service temperature presents a severe limitation in some structural uses of polymers and represents a problem area which is discussed subsequently.

AEROSPACE APPLICATIONS OF POLYMERS AND COMPOSITES

One of the largest materials research efforts on nonmetallic materials is in the field of composite materials, such as the epoxy-glass fibers for filament-wound structures. See references 2, 3, and 4.

Filament-wound structures offer a strength-to-weight ratio which is three times as efficient as that for titanium and four times as high as that for aluminum. In aerospace applications, this strength-to-weight ratio can lead to significant increases in final velocity and in payload weight. Filament-wound structures are considerably more efficient than metals because of the high directional strength of the glass fiber which can be applied in the direction of the load. Metals have isotropic strength properties and require additional weight in the structure to satisfy the maximum unidirectional loads while only part of the strength is used for lesser loads in other directions.

The materials presently used for filament-wound structures are high-strength continuous filaments of E glass held in an epoxy matrix. The resins used in the majority of cases are conventional bisphenol A - epichlorohydrin epoxies. Generally, these resins are cross-linked or cured by addition of an amine
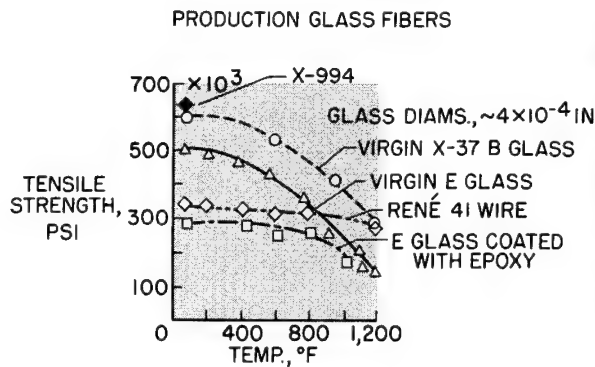
PRODUCTION GLASS FIBERS

FIGURE 68-3.—Tensile strength as a function of temperature.

FIGURE 68-4.—Isotensoid filament-wound rocket case.

hardener. The effect of temperature on the tensile properties of E glass and on an experimental high-temperature glass X-37 B are shown in figure 68-3. (See ref. 2.) The top two curves refer to the glasses alone and the lowest curve applies to the glass-epoxy composite which has a lower service temperature because of the presence of the plastic. René, a superalloy of nickel and cobalt is included for comparison. The highest point (at 650,000 psi) is for a very new high-strength glass, X-994, which holds great promise for future applications.

Research at the NASA Langley Research Center (ref. 5) and in industry (ref. 6) on the isotensoid concept of filament winding has resulted in extremely efficient high strength-to-weight ratio rocket-motor cases. The isotensoid design is based on the concept of designing an equal and uniform tension in each fiber. An example of the isotensoid design is shown in figure 68-4. This case had a burst pressure of 710 psig which represents an overall skin stress of 185,000 psi, or more than twice the usual values for glass-fiber-reinforced cases. Even this advance could be improved upon by using some of the remarkable new glasses, such as X-994, and improved resin systems which would make possible skin stresses as high as 300,000 psi.

The properties of these kinds of materials are at least pragmatically understood for terrestrial applications. Even in the unusual environment experienced by a vehicle during transport into space, our knowledge of materials

properties is adequate because of the short transit time. However, the knowledge of their extended life in space, under the combined influence of the ultravacuum, and ultraviolet, and ionizing radiation is by no means adequate.

ERECTABLE SPACECRAFT

Future programs require knowledge of the long-time effects of the space environment on nonmetallic structural materials. Such projects as erectable space structures and space-storable fuel tanks might be cited as examples. Various designs and materials requirements were discussed at a recent conference on manned space stations (refs. 7 and 8). One space-station design is shown in figure 68-5. This concept calls for the use of an 80-mil Dacron filment-wound torus with an 8-mil butyl-impregnated nylon liner. Such a structure could be easily folded into 2 percent of its inflated volume external to the hub of transport into orbit where it could then be erected pneumatically. This design essentially uses only polymeric materials.

In another space-station design, polymeric materials were used in combination with metals because of their desirable low density and low thermal conductivity. Figure 68-6 shows a cross section of this composite shell in which a foamed polyurethane would serve several purposes, namely, to provide thermal insulation and structural rigidity, and to act as a micro-
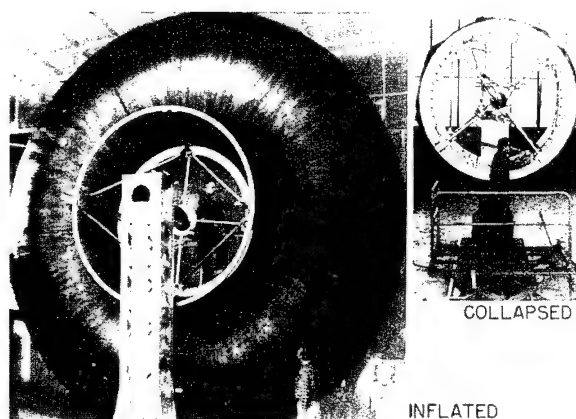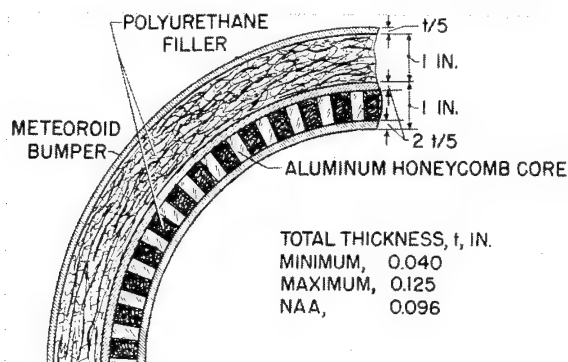
FIGURE 68–5.—24-foot erectable space station.

FIGURE 68–6.—Basic structure of module shell for rigid space station.

meteroid bumper (see ref. 8). The density of a typical foam in this application is approximately 1.5 lb/cu ft.

Another example of the use of polymeric materials in spacecraft design is the giant Echo I sphere which has been in orbit for over 2 years. Echo I was the first passive communications satellite and had a diameter of 100 feet with a skin thickness of 5×10^{-4} inch. This large sphere was made almost entirely of polyethylene terephthalate (Mylar). This polymer is known to be highly resistant to the effects of high-energy ionizing radiation but is rather susceptible to damage from ultraviolet radiation. It was largely protected from the ultraviolet by a 2,200 Å coating of vapor-deposited aluminum. This thin layer of aluminum served several purposes: (1) it provided a radar-reflective surface for the communications experiments; (2) it protected the Mylar from extensive ultraviolet damage; and (3) it acted as a thermal control surface to reduce the equilibrium temperature of the sphere.

THERMAL CONTROL SURFACES

Another use of polymers and other nonmetallic materials in space is as thermal control coatings. The ratio α_s/ϵ, that is, the absorptance of solar radiation divided by the emittance of thermal radiation, is the prime surface parameter which determines surface equilibrium temperature. Figure 68–7 shows the relationship between α_s/ϵ and temperature. Nonmetallic mixtures such as paints have been used to provide the proper optical properties for previous spacecraft surfaces. In this instance, the polymeric vehicle is exposed, virtually unprotected, to the harsh space environment. This exposure has created some problems in the past and a considerable effort has been underway for the past few years to produce stable paints for thermal control coatings. It is generally recognized that inorganic surfaces are inherently more stable than organic surfaces as a result of the nature of the chemical bonds involved.

The NASA Langley Research Center has recently studied an unusually thin, stable inorganic coating known as Alodine 401 for use on A–12 (Echo II), a larger rigidized version of Echo I. This 135-foot sphere required a very light and thin surface coating to cover its nearly 60,000 sq ft of surface. Clemmons and Camp (ref. 9) have reported on the range of the α_s/ϵ
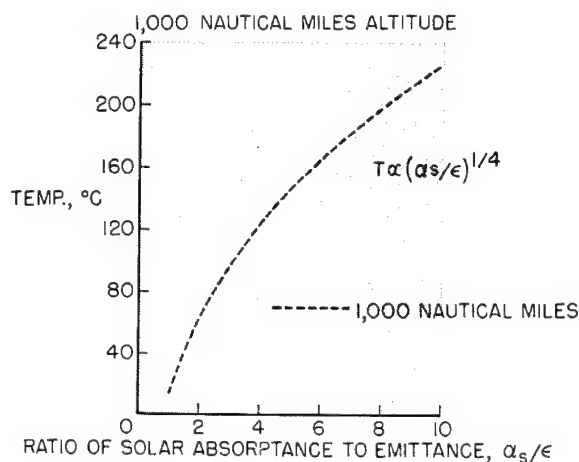

FIGURE 68–7.—Temperature as a function of the ratio of solar absorptance to emittance.
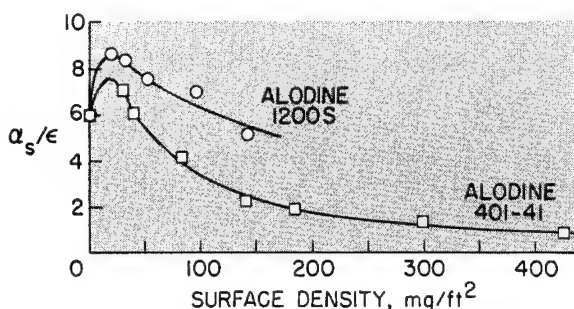
FIGURE 68-8.—Variation of a_s/ϵ with surface density for Alodine coatings.

FIGURE 68-9.—Effects of space environment on polymers.

ratios that can be obtained as a function of surface density of the inorganic Alodine coating; this is illustrated in figure 68–8. The Alodine surface is an amorphous mixture of alumium and chromium phosphates which is formed by reacting pure alumium foil with mixed acids in an aqueous dip process. In addition to its very desirable optical properties, Alodine can be applied easily to a surface, and the surface density can be controlled to within ±3 mg/sq ft.

These have been but a few examples of the uses of polymers and other nonmetallic materials in aerospace applications. There are numerous other uses such as solid-fuel binders, electrical wire insulators, gaskets, and lubricants.

EFFECTS OF SPACE ENVIRONMENT ON POLYMERS

During long-term exposure to the space environment, polymers can undergo many changes in their chemical and resultant mechanical properties. The chemical effects of the space environment on polymers can be classified into three major energy ranges which can act separately or in conjunction with each other. Figure 68–9 illustrates these three energy ranges—the ultravacuum-thermal range, the photochemistry range, and the radiation chemistry range. In the past, engineers have designed around the undesirable effects produced by each of these energy ranges. In the near and long-term future, this luxury will no longer be permitted. Each design must be optimum, and to do this effectively, a better understanding
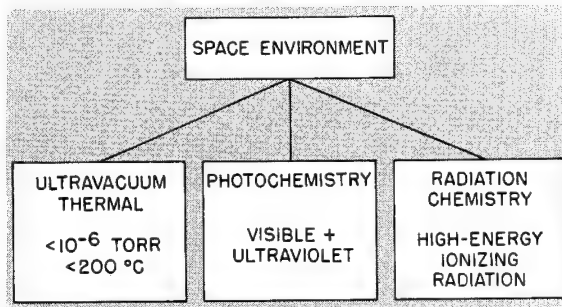
of the properties of materials and their interaction with the space environment must be reached. The recent state of knowledge with regard to the specific qualities and quantities of the high- and low-energy ranges in space is discussed in the preceding paper. The curve in figure 68–10 represents the solar spectrum at one astronomical unit from the sun. The general mechanism of the interaction of radiation with matter will now be considered.

Figure 68–11 represents the spectrum of energies from infrared to high-energy particles; the energy ranges included in thermal chemistry, photochemistry, and radiation chemistry are indicated.

In the infrared region, the energies are associated with vibrational, rotational, and translational motions of molecules, with no alteration of primary chemical bonds—simply an increase in temperature. On the other hand,
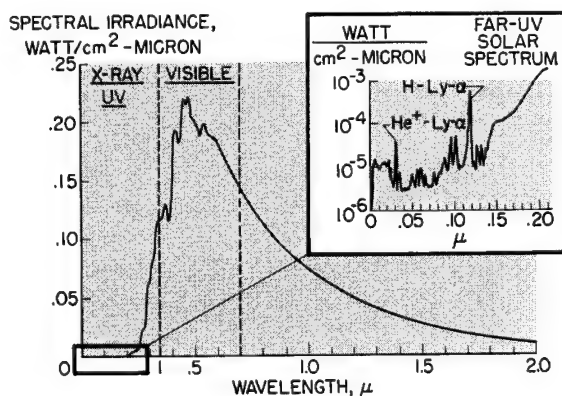

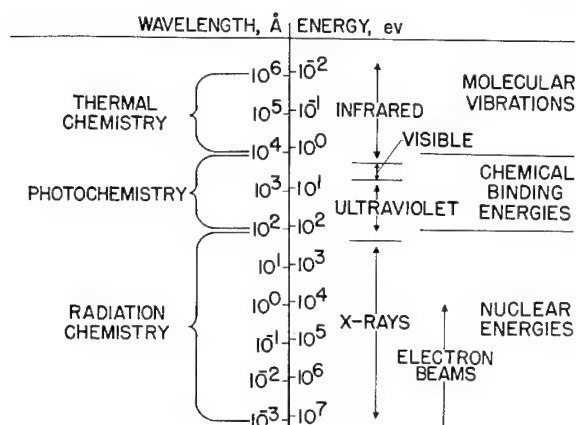FIGURE 68-10.—Solar spectral irradiance at Earth's mean distance from the Sun.

FIGURE 68–11.—Energy spectrum.

FIGURE 68–12.—Effects of vacuum on weight loss of flexible fabric.
$p=5\times10^{-7}$ mm Hg; T=25° C.

in the visible and ultraviolet region, there is considerable making and breaking of bonds, for here the energies involved are of the same order as the energies holding the molecules together. As a consequence, if small amounts of energy are absorbed from this region, they produce significant changes primarily at the surface of the material as this radiation is not very penetrating.

Beyond the ultraviolet range the high-energy ionizing radiation may be corpuscular or electromagnetic in form. These energies are generally much higher than molecular bonding energies and are not limited to surface effects but can penetrate to various depths of the structural material depending on the mass and energy of the radiation.

Ultravacuum-Thermal Region

In the ultravacuum-thermal region, molecular distillation or outgassing is the main effect observed. The gases evolved may come from absorbed molecules or dissociation products produced by higher energies. Jaffee and Rittenhouse (ref. 10) have reviewed the research in this area. A controversy has been developing in the literature for some time with regard to the effects of the ultravacuum-thermal region on polymers. Most of the past data were obtained over relatively short time periods—on the order of days. There is some evidence by Osborne and Goodman (ref. 7) that the experiment should be continued for very long time periods—for weeks and months. This is
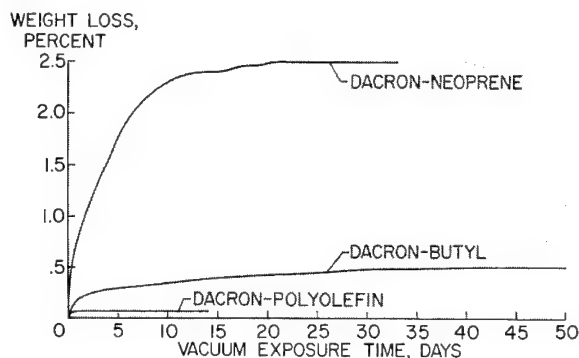
illustrated in figure 68–12 which is a plot of percent weight loss as a function of exposure time for several different materials. Note that the Dacron-Neoprene case requires almost 2 weeks to level off. For the most part, the effects in this low-energy range are of concern primarily from the standpoint of contamination of man and instruments by volatile components.

Visible-Ultraviolet Effects

The effects of the intermediate energies, the visible and ultraviolet radiation, while not highly penetrating, are of particular concern with regard to surface coatings. As mentioned previously, most satellites have some type of thermal control coating on their exterior surfaces. For those satellites which generate heat internally from onboard equipment, it is necessary to have very stable, thermally white surfaces. Here on earth the yellowing of white paints with age is a very familiar phenomenon. In space, this effect is accelerated because there is no atmosphere to filter out the ultraviolet radiation below 3,000 Å. One very stable surface which was discussed previously is the Alodine coating.

Figure 68–13 shows the effect of ultraviolet radiation on this Alodine surface. There is an initial small rise in its α_s/ϵ ratio and then a surprising decrease in this property. This is the reverse of the normal behavior of most thermal control surfaces and means that the equilibrium temperature should decrease somewhat rather than increase with age. Within limits this is desirable.
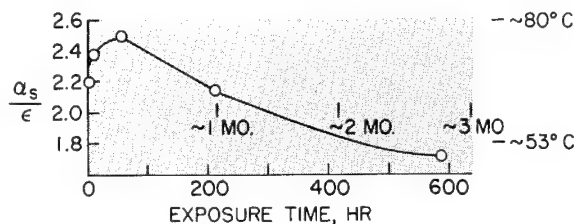
FIGURE 68–13.—Effect of ultraviolet on Alodine 401–41.

The α_s/ϵ ratio is a rather gross property, and to attempt to understand the mechanism of thermal control surfaces, such as Alodine, a more careful examination of basic optical properties must be made. This coating is essentially transparent to solar radiation and, as a result, the shiny opaque substrate of aluminum foil acts to reflect most of this energy away from the spacecraft. However, in the infrared region where the surface radiates away the small amount of energy which is not reflected, the Alodine coating is not transparent to the radiation. This is illustrated in figure 68–14 which shows the percent emittance as a function of wavelength. Note the very low emittance for the uncoated aluminum foil. While there are two major peaks at about 3μ and 9.5μ, respectively, they are not of equal importance. The ideal curve for a 350° K blackbody has its peak at about 9μ and about one-third of the energy is in the 8μ to 12μ region, whereas only a few percent of the total energy of a 350° K blackbody falls around 3μ. Hence, small changes in the 9μ region are much more significant than in the 3μ region. The large peak at 9.5μ for the Alodine 401 is probably due to the molecular vibrations of the phosphate
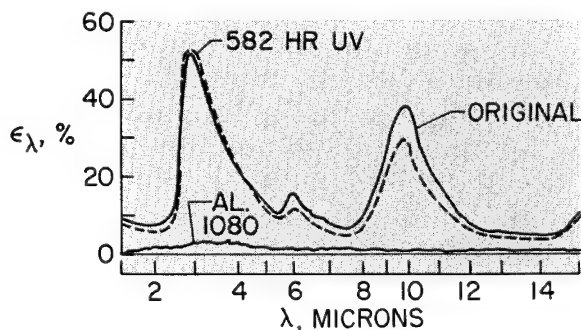

FIGURE 68–14.—Effect of ultraviolet on emittance of Alodine 401–41.

group. Note that after over 500 hours exposure to ultraviolet radiation there is little change in this property. The ultraviolet effects on structural polymers can be largely eliminated by such techniques as using an external opaque surface, for example, the vapor-deposited aluminum coating of Echo I.

Effects of Ionizing Radiation on Polymers

In contrast to photochemical effects, the effects of high-energy ionizing radiations found in space cannot be so easily shielded. These are the effects of the high-energy electrons and protons whose energies and fluxes were discussed in the preceding paper. The radiation chemistry of polymers became an area of intense activity shortly after World War II, and in recent years several review and reference texts have been published in this field (see refs. 11 to 14). The Radiation Effects Information Center at Battelle Memorial Institute maintains abstracts of current information in this field. Most of the past work in radiation effects on polymers has been oriented toward their use here on earth in and near nuclear reactors. As a consequence, many of these studies have been conducted in air and many polymers have been classified as sensitive to radiation. Several principles have been developed during the last decade which indicate some general trends in the effects of radiation on polymers. Some of these are shown in figure 68–15.

In general, addition polymers which have a 1,1 disubstituted repeating unit

$$\left(-CH_2-C{<}^X_Y\right)$$
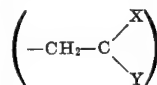
have been shown to degrade under the influence of ionizing radiation. Those addition polymers which have only a single substitution

$$\left(^{CH_2-CH}{\diagdown}_X\right)$$
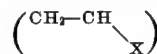
on alternate carbons generally cross-link under irradiation. It is also recognized that polymers with benzene rings such as polystyrene and Mylar are resistant to radiation effects because the unsaturated ring acts as an energy sink and absorbs energy without degrading the polymer. While these are general rules, they
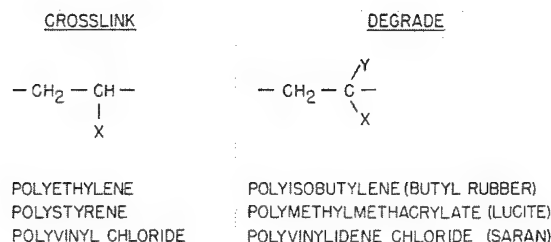
FIGURE 68–15.—Radiation effects on polymers.

FIGURE 68–17.—Effect of γ irradiation on the tensile strength of fluorocarbon plastics.

do not cover a large number of other polymers such as the polycarbonates, polyacetals, and epoxies. It has been necessary therefore to treat these others as separate cases and to determine their behavior directly. One must exercise extreme caution so as not to misapply the wealth of background in radiation effects on polymers in air to their reactions in space. This is also true even for reported work in vacuo inasmuch as the degree of vacuum can play an important role. Vacuum work should be carried out at a continuous pressure of 10^{-5} or 10^{-6} torr as a maximum in order to reduce the concentration of oxygen and other reactive gases. Figures 68–16 and 68–17 illustrate the drastic difference between irradiation in air and in vacuo for some polyfluorocarbons (see ref. 15).
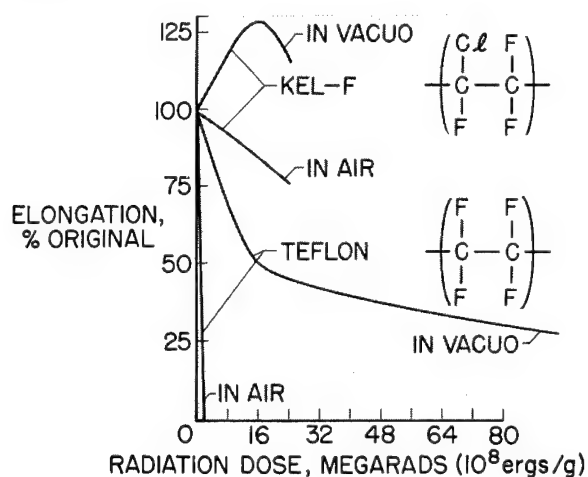

FIGURE 68–16.—Effect of γ irradiation on the elongation of fluorocarbon plastics.

NEW MATERIALS RESEARCH

High-temperature environments represent another problem area which calls for increased research effort. Some of the details of one
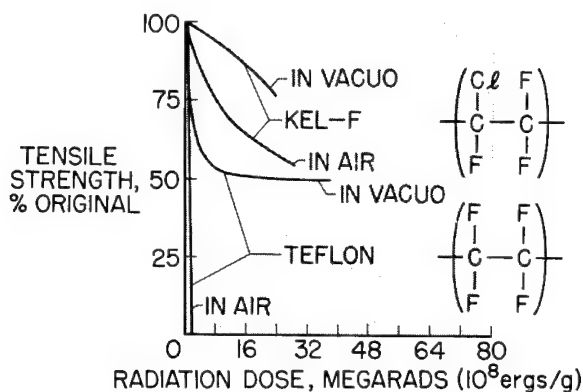
high-temperature problem area, namely, reentry, are discussed in the paper by Roberts. There are many cases which require materials with high-temperature stability. In synthesizing polymeric materials, it is often possible to design specific properties into the molecular structure. This is readily apparent by recalling the dozens of new polymers with a wide range of properties, which reach production each year. One property design, thermal stability, is the goal of extensive polymer research which is now in progress in various university and government laboratories. This work is oriented toward tailor-making high temperature polymers. This research no longer deals with classical organic molecules as building blocks but reaches out to include inorganic materials. This work is still in the very early stages of development. The materials can be classed as inorganic polymers and compound organic-inorganic polymers.

Probably one of the most notable inorganic polymers is the whole family of high-temperature silicone resins which have an Si-O-Si-O backbone in the main chain, though they do contain carbon in side groups. Most of the familiar organic polymers have relatively simple repeating units making up the molecular chain. This is the case with a few inorganic polymers but, in general, the repeating units are somewhat more complex. One example of a simple inorganic polymer is the phosphonitrilic linear polymer made up of P, N, and Cl. Its structure is shown in figure 68–18 and is somewhat reminiscent of the polyisobutylene

PHOSPHONITRILIC LINEAR POLYMER

+ HIGH TEMP. PROPERTIES (300° C)
+ ELASTOMER
−− CHEMICAL STABILITY (HYDROLYSIS)

POLYISOBUTYLENE (BUTYL RUBBER)

−− HIGH TEMP. PROPERTIES
+ ELASTOMER
++ CHEMICAL STABILITY

FIGURE 68–18.—Organic vs. inorganic elastomers.

M = METAL

CHELATE POLYMER

GOOD THERMAL STABILITY IN AIR

MOLECULAR WEIGHTS OVER 10,000
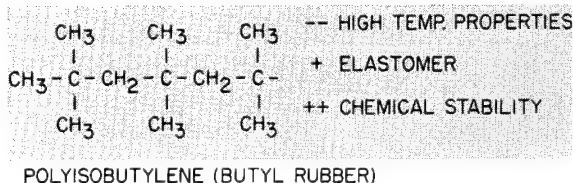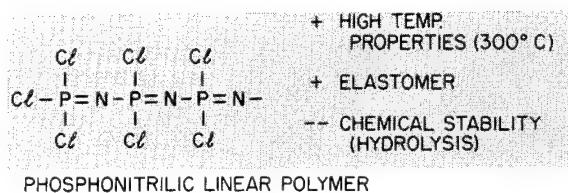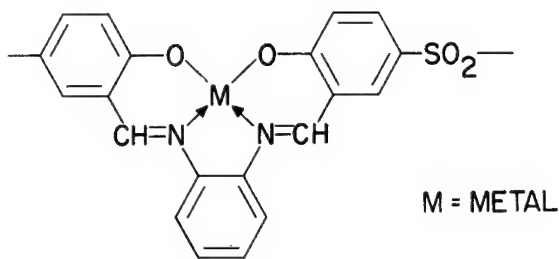
FIGURE 68–19.—Metal-organic polymer.

structure of butyl rubber. The P, N, Cl polymer has been made in the form of oils, waxes, elastomers, and infusible solids. The elastomer has been of special interest as a thermally stable rubber at temperatures on the order of 300° C. Molecular weights from 20,000 to 80,000 have been reported. However, physical and thermal stability are only a part of the picture, chemical stability is also an important factor. The polymer cannot be used here on earth because of its susceptibility to hydrolysis, although in spacecraft applications, where likelihood of hydrolysis is greatly reduced, it may find some specialized use.

Another example of some work on high-temperature polymers is that of C. S. Marvel at the University of Arizona who has prepared a number of complex chelate polymers, one of which is shown in figure 68–19. These are stable from 300° C to 500° C in air and have been made with molecular weights of over 10,000. Many serious problems still exist before this family of polymers will find application. One of the most severe problems is difficulty of processing or fabrication. Often these materials are like a fine glass powder when formed in the reactor and cannot be processed. At present this is one of the unresolved, though not necessarily insurmountable, problems.

CONCLUDING REMARKS

Nonmetallic materials, particularly polymers, have many unusual and desirable properties for use in spacecraft applications, but their sensitivities to ultraviolet and high-energy ionizing radiation of space have created problems—some as yet unsolved. The interaction of the space environment with these materials used in composite form and for thermal control surfaces has been discussed with relation to the present state of knowledge. The need for new nonmetallic materials with properties such as those of inorganic polymers has been discussed. In view of these desirable properties, it has been predicted (ref. 16) that by 1970, one-half of the structural weight of all aerospace vehicles will be fabricated of some form of polymers.

REFERENCES

1. PECKNER, D., and RILEY, M. W.: Metals vs Plastics. Materials in Design Engineering, vol. 55, no. 3, Mar. 1962, pp. 131–142.
2. LAYTON, PAUL: Review of Various Glass Filaments. Filament Winding Conference, March 28–30, 1961, Soc. Aerospace Material and Process Eng., 1961, pp. 197–204.
3. ANON.: Seventeenth Annual Technical and Management Conference (Chicago), Feb. 1962. Secs. 1–A—1–E and Secs. 10—10–E. Sponsored by Soc. Plastics Ind., Inc.
4. PETERSON, GEORGE P.: High Modulus Glass Fibers For Reinforced Plastics. WADD Tech. Rep. 60–735, U.S. Air Force, Sept. 1961. (Available from ASTIA as AD 268902.)

5. LEWIS, D. J., MODISETTE, J. L., and THIBODAUX, J. G.: High Mass Fraction Solid-Propellant Rocket Design Concept. Bulletin of the 18th Meeting—JANAF–ARPA–NASA Solid Propellant Group, Vol. 1, Appl. Phys. Lab., Johns Hopkins Univ., June 1962, pp. 237–260.

6. LEVENETZ, BORIS: Development of an Ultralight Rocket Motor Case. Bulletin of the 18th Meeting—JANAF–ARPA–NASA Solid Propellant Group, Vol. 1, Appl. Phys. Lab., John Hopkins Univ., June 1962, pp. 277–287.

7. OSBORNE, ROBERT S., and GOODMAN, GEORGE P.: Materials and Fabrication Techniques for Manned Space Stations. A Report on the Research and Technological Problems of Manned Rotating Spacecraft. NASA TN D–1504, 1962, pp. 45–58.

8. ZENDER, GEORGE W., and DAVIDSON, JOHN R.: Structural Requirements of Large Manned Space Stations. A Report on the Research and Technological Problems of Manned Rotating Spacecraft. NASA TN D–1504, 1962, pp. 33–44.

9. CLEMMONS, DEWEY L., JR., and CAMP, JOHN D.: Amorphous Phosphate Coatings For Thermal Control of Echo II. Paper presented at the Multilayer Systems Symposium of the Electrochemical Society Meeting (Los Angeles, Calif.), May 6–10, 1962.

10. JAFFEE, L. D., and RITTENHOUSE, J. B.: Behavior of Materials in Space Environments. Tech. Rep. No. 32–150 (Contract No. NASw–6), Jet Propulsion Lab., C.I.T., Nov. 1, 1961.

11. CHARLESBY, A.: Atomic Radiation and Polymers. Pergamon Press (New York), 1960.

12. BOVEY, FRANK A.: The Effects of Ionizing Radiation on Natural and Synthetic Polymers. Interscience Publ., Inc. (New York), 1958.

13. CHAPIRO, ADOLPHE: Radiation Chemistry of Polymeric Systems. Interscience Publ. Inc. (New York), 1962.

14. LIND, SAMUEL C.: Radiation Chemistry of Gases. Reinhold Publ. Corp. (New York), 1961.

15. BRINGER, ROBERT P.: Fluorocarbon Plastics Under the Influence of Unusual Environmental Conditions. Symposium on Effects of Space Environment on Materials. Soc. Aerospace Materials and Process Eng., May 1962.

16. ANON.: Aerospace Age: Plastics in Orbit. Modern Plastics, vol. 139, no. 6, Feb. 1962, pp. 74–79, 152–164.

Ablation Materials for Atmospheric Entry

By Leonard Roberts

DR. LEONARD ROBERTS, *Head, Mathematical Physics Branch, Theoretical Mechanics Division, NASA Langley Research Center, received his Bachelor of Science and Doctorate degrees in the fields of aerodynamics, fluid mechanics, and applied mathematics from the University of Manchester, England, in 1952 and 1955, respectively. From 1955 to 1957 he performed post-doctorate research at the Massachusetts Institute of Technology on problems of heat transfer and mass ablation from bodies in extremely high temperature flows.*

Dr. Roberts joined the Langley staff in June 1957, and has become one of the leading experts in this country in the complex area of analysis of reentry heat shielding by mass ablation. His report prepared while at Massachusetts Institute of Technology on a study of aerodynamic melting is considered a pioneer effort in this subject. In the field of aerodynamic cooling by means of boundary-layer injection and material ablation, Dr. Roberts has published many original papers and has served as a consultant to industry and government agencies. He presented a paper "Radiation and Ablation Cooling for Manned Reentry Vehicles" in Zurich, Switzerland, in September 1960, before the Second International Congress of the Institute of the Aerospace Sciences. His most recent efforts concern the problem of rocket-exhaust—dust-layer interaction during a lunar landing and he presented a paper entitled "Exhaust Jet-Dust Layer Interaction During a Lunar Landing" at the Thirteenth Congress of International Astronautical Federation at Varna, Bulgaria, in September 1962. He has served on several technical committees at Langley and is the author of several NASA publications and other documents.

SUMMARY

Some of the more important concepts of thermal protection by ablation are described and the extent of our progress in ablation materials research is discussed.

A short summary of the thermal environment is given, followed by a discussion of the several ablation processes with particular emphasis on charring ablation. The problem of environment simulation is then discussed and examples of typical facilities presented. Finally, some of the materials that have been successfully flight tested are reviewed.

INTRODUCTION

When a vehicle enters the earth's atmosphere, it has a large amount of kinetic energy which must be disposed in a controlled manner if the vehicle is to survive. A large fraction of this energy is transferred to the atmosphere (as kinetic and heat energy); nevertheless, the remainder, which appears as the aerodynamic heat input to the vehicle, is of such magnitude that its disposal constitutes a major problem.

The limited capability of metals to absorb or to radiate this heat has led to the use of ablation materials—materials which continue to perform in a satisfactory way under conditions of extreme heating. In the 7 years since the use of ablation materials was first given serious consideration as a means of protecting vehicles entering the atmosphere, a large research and

development effort has been applied to the problem of producing, testing, and proving these materials for use in flight.

This paper will describe some of the more important concepts of thermal protection by ablation and at the same time relate the extent of progress in ablation materials research.

THE THERMAL ENVIRONMENT

The motion and heating of vehicles entering the earth's atmosphere has been the subject of continued study for many years and a large amount of information on the flight environment is available. (See, for example, refs. 1 to 5.) The magnitude of the heating problem for vehicles entering the atmosphere is illustrated in figure 69–1.

During entry, the vehicle experiences a heating rate which increases (as the atmospheric density increases) to a maximum value and then decreases as the vehicle is slowed down by atmospheric drag. This maximum value is plotted as the abscissa (fig. 69–1) from 10 to 10^4 Btu/sq ft/sec. The total heat flux experienced by the vehicle during the entry is plotted as the ordinate from 10^3 to 10^6 Btu/sq ft. The hatched line indicates the limits to which metallic heat shields can operate: a molybdenum shield can radiate about 40 Btu/sq ft/sec and a copper heat shield, such as that used on the early ballistic missiles, becomes so heavy that it is unfeasible for heat inputs greater than 10,000 Btu/sq ft. The broad arrow shows the thermal region in which the present and future entry vehicles will operate—the upper half of the arrow corresponds to manned vehicles, the lower

half, to unmanned vehicles which experience a shorter duration of heating. The direction of the arrow is that of increasing entry velocity. It is clear from figure 69–1 that ablation materials play an extremely important role in the protection of vehicles returning from space.

ABLATION CONCEPTS

The success of the ablation shield results first from the fact that it is not heating-rate limited, and second from its ability to dispose of a large amount of heat for a small amount of material loss. In general, the material may undergo sublimation or depolymerization (as is the case with most thermoplastic materials) or melting and vaporization (quartz is a good example of this). Analytical and experimental studies of these forms of ablation are to be found in references 6 to 10. Alternatively, pyrolysis may take place as with thermosetting plastics such as the phenolic resins. (See, for example, refs. 11 to 18.) Examples of the process of heat disposal by some of these materials are shown in figure 69–2.

A ceramic ablation shield is illustrated on the left of this figure. Aerodynamic heating of the virgin material causes it to flow as a liquid near the surface and part of this liquid layer is subsequently vaporized and is transported away by the airstream over the vehicle surface. The quartz ablation shield, presently used on the ICBM nose cone (ref. 19), behaves in this way. During ablation, heat is dissipated as latent heat in the phase change and is also transported away from the surface by convection in the liquid and gas layers.
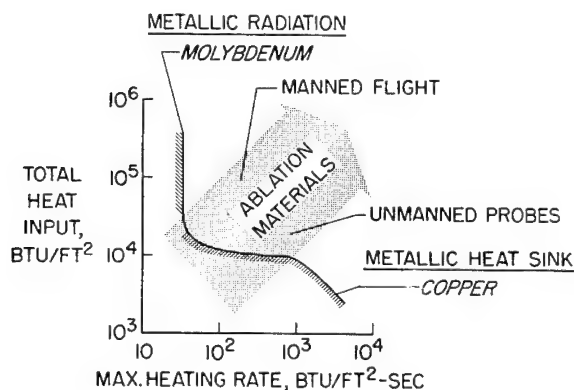

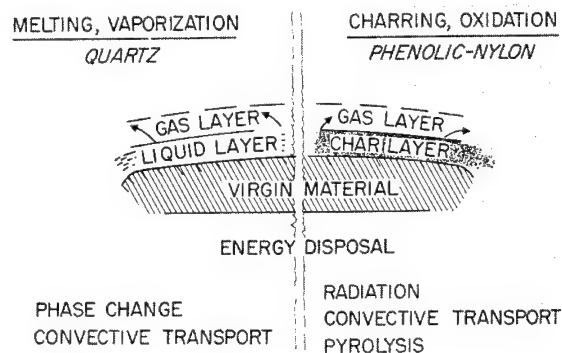
FIGURE 69–1.—Entry-vehicle heating environment.

FIGURE 69–2.—Ablation concepts for two types of material.

On the right of figure 69-2 is illustrated a charring ablation shield. In this case the shield may comprise a resinous material reinforced with glass or nylon. Pyrolysis of the virgin material produces a carbonaceous char which can sustain high surface temperatures. Heat energy is disposed by radiation from the surface, by convective transport, and by pyrolysis within the material.

The capability of the ablation material to dispose of heat cannot be defined without reference to the conditions of heating. The enthalpy of the airstream and the type of heating encountered (whether convective or radiative heating) may play an important part in the response of the material. Radiative heating (refs. 20 to 22) becomes important when the air passing over the vehicle is sufficiently hot to radiate heat energy.

The effects of these environmental conditions are illustrated in figure 69-3. On the left is shown the variation, with the stream enthalpy, of a heat-disposal parameter H measured in Btu/lb for two materials, quartz and Teflon, under conditions of negligible radiation. It is seen that the relation is approximately linear. For example, the intercept on the Teflon curve at H=1,000 Btu/lb represents the latent heat of depolymerization of the material. The subsequent increase in H above this value with increase in stream enthalpy represents the additional heat absorbed by the gaseous products as they are transported away from the surface. It is evident that the material behaves very efficiently when the stream enthalpy is large, or equivalently, when the vehicle is traveling at high speed (since the stream enthalpy is an indication of the vehicle kinetic energy).

The right-hand side of figure 69-3 shows the additional effect of radiation. The broken line is the basic curve for no radiation, the upper line shows the enhanced performance when radiative cooling occurs, and the lower line shows the poorer response of the material to radiative heating. The hatched areas indicate the experimental results on each of these curves.

From figure 69-3 one would conclude that the high-temperature materials which allow the benefits of radiation cooling are superior. This
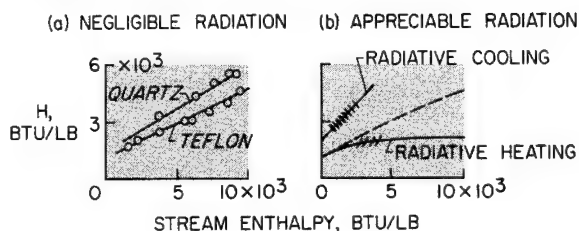

FIGURE 69-3.—Effects of environmental conditions on heat-disposal capability.

is not always the case, however, since the high-temperature materials also encourage conduction of heat to the cool structure and therefore introduce a severe insulation problem. This problem is especially important for manned vehicles since they tend to endure longer periods of heating. Therefore, the characteristic conduction time for the material must be considered since this time provides an indication of the insulative quality of the material.

The surface temperature of the material and the characteristic heat conduction time are the two quantities which determine its insulative capability; these two quantities are plotted along the ordinate and the abscissa, respectively, of figure 69-4. For the purposes of this paper, the characteristic conduction time is the time required for the temperature at the back surface of a slab, 5 lb/sq ft in thickness, to increase by 300° F when the front surface is raised to the indicated temperature. The characteristic conduction times for various types of material are presented in this figure.

The first noticeable result is that the high-temperature materials have low characteristic conduction times. Graphite, for example, is capable of sustaining very high temperatures and can dispose of large amounts of heat under
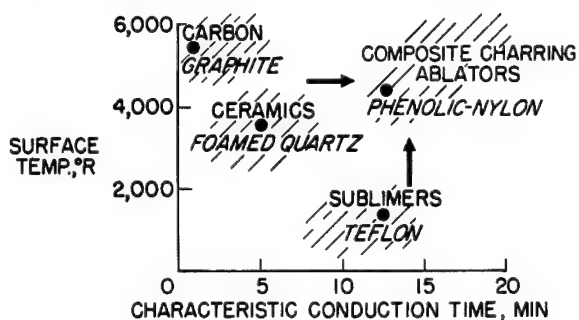

FIGURE 69-4.—Insulation capability of various materials.

severe heating conditions. Its characteristic conduction time, however, is extremely low; thus, it cannot be used when it is necessary for the vehicle to remain cool for a long period of time, although it may be used at isolated locations far removed from the cool structure.

The low-temperature subliming materials, on the other hand, have a much longer characteristic conduction time and thus reduce the problem of insulation. However, they cannot radiate appreciably and may suffer a large amount of ablation over long heating periods. Ceramics, as a class, tend to fall between these two extremes.

Evidently, the ideal material is capable of radiating at high surface temperatures and at the same time has a long characteristic conduction time so that heat penetrates through the material very slowly. The ideal material has not yet been found, of course, but some progress in this direction has been made in recent years in the development of composite charring materials. These materials, in the virgin state, have good insulative properties but during ablation produce a carbonaceous char which attains a high surface temperature and therefore radiates an appreciable amount of heat.

CHARRING ABLATION

A typical composite ablation material consists of a phenolic or an epoxy resin reinforced with fiberglass or asbestos in the form of random or oriented fibers or in the form of a cloth. The ablation shield used on the Mercury spacecraft, for example, was a combination phenolic-fiberglass material. Figure 69–5 illustrates the several phenomena that take place simultaneously during the ablation of such a material. The material is shown in several layers; at the lower part of the figure is the virgin material which is attached to the structure. Above the virgin material is a pyrolysis zone in which the phenolic resin starts to pyrolyze and form a char which accumulates to form a thick layer supported by the reinforcing material. The exposed surface of this reinforced char undergoes melting and oxidation and these two effects, together with aerodynamic shear and pressure forces, limit the growth of the char layer. Within the char, conduction of heat inwards to the pyrolysis zone is partly canceled by the transpiration of gases outward to the surface, and the subsequent introduction of these gases into the external flow provides further cooling. Since the char has a high carbon content, it sustains high surface temperatures and radiates an appreciable amount of heat. However, since pyrolysis takes place at a relatively low temperature, little conduction of heat takes place within the virgin material. This type of ablation has been investigated both experimentally and theoretically and appears to promise the solution to the heating problem encountered by manned entry vehicles. (See refs. 23 and 24.)

The evaluation of charring materials is made particularly difficult by the fact that several effects take place simultaneously, and a thorough understanding of the effects of extreme heating requires both experimental and theoretical research on the ablation mechanism. There are three major areas of research that require attention.

First, more complete information is needed on the chemistry that describes char formation. It is known experimentally that hydrogen and oxygen atoms are stripped from the phenolic structure at high temperatures, but there is still room for a more complete quantitative description of the reactions that take place throughout the char and of the way in which the internal transport of heat and chemical species affect these reactions. Second, information on char-layer properties is required, especially at high temperatures. Such properties as the surface emissivity, the thermal conductivity, porosity,

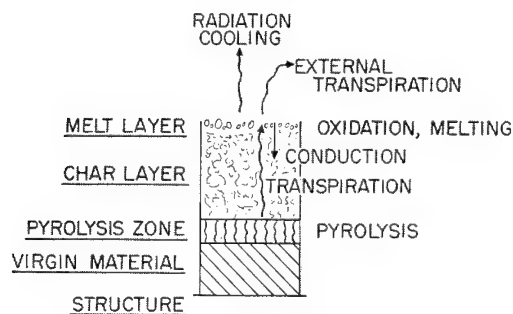*PHENOLIC-NYLON; PHENOLIC-ASBESTOS; PHENOLIC-GLASS*

FIGURE 69–5.—Composite charring ablation phenomena.

and resistance to shear and pressure forces are all important in determining its response to the environment of atmospheric entry. Last, information on the interaction of the products of ablation with the aerodynamic flow over the surface of the vehicle is needed. Chemical reactions at the surface and in the gas boundary layer may change the chemical and physical character of the flow to such an extent that appreciable changes in the heating rate may result, and these changes will then feed back and modify the response of the material.

Although these problems do not involve new concepts, they are nevertheless complex and are of such a nature that the researcher requires a background in two or three disciplines.

SIMULATION OF THE HEATING ENVIRONMENT

Since the behavior of ablation materials depends so much on the environmental inputs, the heating rate, stream enthalpy, shear stress, and so forth, it is not always easy to extrapolate from laboratory experiments up to flight conditions, and it is rarely possible to simulate the several environmental effects which control the ablation process. Accordingly, in the planning of experimental tests, the primary inputs must be determined and provision made for their proper simulation while the less important ones must be abandoned. The environmental factors of most importance in one kind of ablation, however, are not necessarily important in another.

For materials that sublime or depolymerize, the stream enthalpy and the percentage radiative heating are important. For materials which melt at a high temperature, however, the total heat input, which determines the rate of production of the melt, and the shear stress, which governs the rate of removal of the melt, are the primary inputs. The stream enthalpy continues to be important. When ablation by charring takes place, char is produced by heating and removed by oxidation and by shear and pressure forces; therefore, these quantities must be simulated.

Experimental research on such materials has been carried out in a variety of facilities. (See refs. 12 and 25 to 30.) These facilities include the relatively simple oxyacetylene torch which
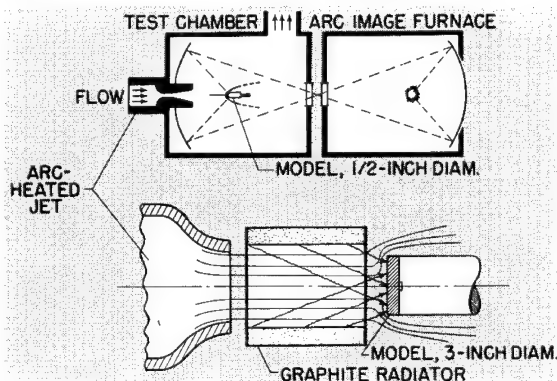

FIGURE 69-6.—Two types of reentry heating simulator.

has been used primarily as a means of screening materials, the rocket-motor exhaust, electric-arc tunnels, and the graphite furnace and arc-image furnace which produce a radiation-heating environment.

Figure 69-6 shows two facilities which simulate both the convective and radiative heating environment associated with high-speed entry into the atmosphere. In the upper half of the figure is shown a schematic diagram of the combined convective-radiative heating facility at the NASA Ames Research Center. (See ref. 30.) An arc-type heater supplies the hot air which passes through the nozzle and over the model to provide convective heating. Radiative heating is supplied by a carbon-arc lamp whose radiation is focused on the face of the model by the use of two elliptical mirrors as shown. The convective heater produces a heating rate up to 600 Btu/sq ft/sec (on a model with a nose radius of $3/8$ inch) and a stream enthalpy up to 7,000 Btu/lb. The arc-image furnace produces heating rates up to 750 Btu/sq ft/sec when operating on a power source of 300 amperes at 75 volts.

The lower half of the figure shows a reentry heating facility at the Langley Research Center. (See ref. 28.) Again convective heating is supplied by an arc-heated airstream, but the radiative heating is supplied by a graphite radiator. In this facility 3-inch-diameter specimens have been subjected simultaneously to convective heating rates of 200 Btu/sq ft/sec at a stream enthalpy of 3,500 Btu/lb and varying radiative heating rates up to 200 Btu/sq ft/sec. The experimental results obtained from these facilities, together with some ana-
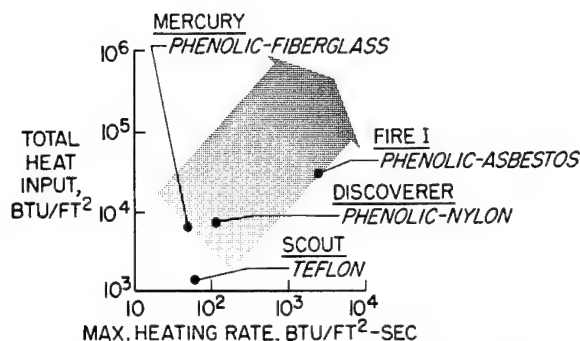
FIGURE 69–7.—Flight-tested ablation materials.

lytical work, have provided a better understanding of the ablation of charring materials under conditions of extreme heating.

FLIGHT TESTS

Despite the large experimental efforts applied to the evaluation of ablation materials in ground facilities, it is never possible to duplicate the complete flight environment, and flight testing is always necessary before the material can be approved for operational use. During the last few years, an increasing amount of information has been obtained from recovered entry vehicles. Figure 69–7 shows some of the materials that have been tested and the vehicles used. The variables are those used in figure 69–1, the total heat input per unit area and the maximum heating rate per unit area. It is seen that the flight tests fall generally within the broad arrow that was shown in figure 69–1.

The Scout vehicle has been used to determine the flight performance of Teflon on a short-duration suborbital entry. The Mercury spacecraft has demonstrated the flight worthiness of the phenolic-fiberglass charring ablation shield. Similarly, the unmanned Discoverer satellite entered the atmosphere successfully with a phenolic-nylon ablation shield and a melting ceramic shield has also proved successful on the Titan ICBM nose cone. Future flight plans by NASA include Project Fire which will investigate aerodynamic conditions at speeds up to 40,000 ft/sec and will probably use a phenolic-asbestos charring ablation shield. Much of this information will be useful in deciding the type of ablation shield to be used on future spacecraft.

There is still a large area within the arrow that has not yet been covered by flight tests; this region corresponds to flights of relatively long duration (20 to 40 minutes) and such flights cannot be made with a simple ballistic vehicle but require a more sophisticated vehicle having aerodynamic lift. In view of the importance of this longer duration heating environment to manned atmospheric entry, it is likely that this area will receive increased attention in future flight tests.

CONCLUDING REMARKS

Considerable advances have been made in the technology of ablation in a relatively short period of time. This is not to say, however, that all the answers have been obtained, and there is a large continuing effort in this field. The need to produce lightweight versatile ablation materials still exists and future research and development will be directed toward materials that have a high heat-disposal capability and, at the same time, good insulative qualities and mechanical strength. Further, these materials must be easily applied to large surface areas if they are to protect vehicles having aerodynamic lift capability.

Clearly, the progress already made has been significant and, in view of the operational success of ablation materials on the Mercury spacecraft and other vehicles, the ablation approach appears to be the most satisfactory one for the protection of future vehicles returning from space.

REFERENCES

1. ALLEN, H. JULIAN, and EGGERS, A. J., JR.: A Study of the Motion and Aerodynamic Heating of Ballistic Missiles Entering the Earth's Atmosphere at High Supersonic Speeds. NACA Rep. 1381, 1958. (Supersedes NACA TN 4047.)
2. CHAPMAN, DEAN R.: An Approximate Analytical Method for Studying Entry Into Planetary Atmospheres. NASA TR R–11, 1959. (Supersedes NACA TN 4276.)
3. GAZLEY, CARL, JR.: Deceleration and Heating of a Body Entering a Planetary Atmosphere From Space. Vol. I of Vistas in Astronautics, Morton Alperin, Marvin Stern, and Harold Wooster, eds., Pergamon Press, c. 1958, pp. 8–32.
4. LOH, W. H. T.: Dynamics and Thermodynamics of Re-Entry. Jour. Aerospace Sci., vol. 27, no. 10, Oct. 1960, pp. 748–762.
5. GOODWIN, GLEN, and CHUNG, PAUL M.: Effect of Nonequilibrium Flows on Aerodynamic Heating During Entry Into the Earth's Atmosphere From Parabolic Orbits. Advances in Aero. Sci., vols. 3–4, Pergamon Press (New York), 1961.
6. SUTTON, GEORGE W.: The Hydrodynamics and Heat Conduction of a Melting Surface. Jour. Aero. Sci., vol. 25, no. 1, Jan. 1958, pp. 29–32, 36.
7. ROBERTS, LEONARD: On the Melting of a Semi-Infinite Body of Ice Placed in a Hot Stream of Air. Jour. Fluid Mech., vol. 4, pt. 5, Sept. 1958, pp. 505–528.
8. LEES, LESTER: Similarity Parameters for Surface Melting of a Blunt Nosed Body in a High Velocity Gas Stream. ARS Jour., vol. 29, no. 5, May 1959, pp. 345–354.
9. BETHE, HANS A., and ADAMS, MAC C.: A Theory for the Ablation of Glassy Materials. Jour. Aero/Space Sci., vol. 26, no. 6, June 1959, pp. 321–328, 350.
10. ROBERTS, LEONARD: Stagnation-Point Shielding by Melting and Vaporization. NASA TR R–10, 1959.
11. ADAMS, MAC C.: Recent Advances in Ablation. ARS Jour., vol. 29, no. 9, Sept. 1959, pp. 625–632.
12. LEES, LESTER: Convective Heat Transfer With Mass Addition and Chemical Reactions. Presented at Third Combustion and Propulsion Colloquium of AGARD (Palermo, Sicily), Mar. 17–21, 1958.
13. GRUNTFEST, I. J., and SHENKER, L. H.: Behavior of Reinforced Plastics at Very High Temperatures. Modern Plastics, vol. 35, no. 6, June 1958, p. 55.
14. BARRIAULT, R. J., and YOS, J.: Analysis of the Ablation of Plastic Heat Shields That Form a Charred Surface Layer. ARS Jour., vol. 30, no. 9, Sept. 1960, pp. 823–829.
15. SWANN, ROBERT T., and PITTMAN, CLAUD M.: Numerical Analysis of the Transient Response of Advanced Thermal Protection Systems for Atmospheric Entry. NASA TN D–1370, 1962.
16. SCALA, SINCLAIRE M., and GILBERT, LEON M.: The Thermal Degradation of a Char-Forming Plastic During Hypersonic Flights. ARS Jour., vol. 32, no. 6, June 1962, pp. 917–924.
17. BROOKS, WILLIAM A., JR., SWANN, ROBERT T., and WADLIN, KENNETH L.: Thermal Protection for Spacecraft Entering at Escape Velocity. [Preprint] 513F, Soc. Automotive Eng., Apr. 1962.
18. SCHMIDT, DONALD L.: Ablation of Plastics. ASD–TR–61–650, U.S. Air Force, Feb. 1962.
19. YAFFEE, M.: Ablation Wins Missile Performance Gain. Aviation Week and Space Technology, vol. 73, no. 3, 1960, pp. 54–55, 57, 59–61, 65.
20. MEYEROTT, R. E.: Radiation Heat Transfer to Hypersonic Vehicles. Lockheed Rep. LMSD 2264, Lockheed Aircraft Corp., Nov. 1957.
21. KIVEL, B., and BAILEY, K.: Tables of Radiation From High Temperature Air. Res. Rep. 21 (Contracts AF 04(645)–18 and AF 49(638)–61), AVCO Res. Lab., Dec. 1957.
22. TEARE, J. D., GEORGIEV, S., and ALLEN, R. A.: Radiation From the Non-Equilibrium Shock Front. Res. Rep. 112 (Contract AF 19(604)–7458), AVCO Res. Lab., Oct. 1961.
23. ROBERTS, LEONARD: Radiation and Ablation Cooling For Manned Re-Entry Vehicles. Advances in Aero. Sci., vols. 3–4, Pergamon Press (New York), 1961, pp. 1019–1044.
24. STEG, LEO: Materials for Re-Entry Heat Protection of Satellites. ARS Jour., vol. 30, no. 9, Sept. 1960, pp. 815–822.
25. LUCAS, WILLIAM R., and HUSTON, MYRON E.: Planning a Re-Entry and Recovery Test Program. Astronautics, vol. 4, no. 3, Mar. 1959, pp. 30–31.
26. ANON.: Determination of Factors Governing Selection and Application of Materials for Ablation Cooling of Hypervelocity Vehicles. CML–TN–M131–11 (Contract No. AF 33(616)–5436), Chicago Midway Labs., Univ. of Chicago, 1958.

27. GEORGIEV, STEVEN, HIDALGO, HENRY, and ADAMS, MAC C.: On Ablation for the Recovery of Satellites. Res. Rep. 47 (Contract AF 04(647)–278), AVCO Res. Lab., Mar. 6, 1959.

28. WADLIN, KENNETH L., and KOTANCHIK, JOSEPH N.: The Use of Ablators for Achieving Protection Against High Thermal Flux. [Preprint] 417C, Soc. Automotive Eng., Oct. 1961.

29. SAVIN, RAYMOND C., GLORIA, HERMILO R., and DAHMS, RICHARD G.: The Determination of Ablative Properties of Materials in Free-Flight Ranges. NASA TN D–1330, 1962.

30. LUNDELL, JOHN, WINOVICH, WARREN, and WAKEFIELD, ROY: Simulation of Convective and Radiative Entry Heating. Presented at Second National Symposium on Hypervelocity Techniques (Denver, Colorado), Mar. 19–20, 1962.

Flow and Fracture Problems in Aerospace Vehicles

By Richard H. Kemp

RICHARD H. KEMP, *Head of the Powerplant Structures Section of the NASA Lewis Research Center, has specialized in stress and vibration research in propulsion structures. A native of Genoa, Ohio, Mr. Kemp is a graduate of the University of Toledo where he received his bachelor of engineering degree in 1943. He is a member of the Society for Experimental Stress Analysis, a member of the American Rocket Society, and a licensed Professional Engineer of the State of Ohio.*

INTRODUCTION

Critical weight requirements for aerospace vehicles make it mandatory that each structural component bear its share of the imposed loads and operate at stress levels very close to the strength limits of the material. Such operation requires working with safety factors that are considerably smaller than those usually used. For example, a safety factor of 1.2 on the yield strength is not uncommon in the design departments of major space vehicle manufacturers. The use of such low safety factors requires, first, that the loads on the vehicle be precisely known, and, second, that the reaction of the material to a given situation of loading and environment be known or predictable. For the purposes of this discussion, it is assumed that the loads and stress distribution have been satisfactorily determined. (They can not always be determined, though, primarily because of unknown dynamic loads.) It remains to establish the capability of the given material in some component form to carry this load and stress distribution in the most efficient manner, despite the fact that materials are never perfect and will generally contain flaws or defects that establish some limit to their use.

As a result of utilizing materials at stress levels close to their maximum capability, it becomes exceedingly important to arrive at an under-standing of their basic behavior when loaded. In conducting basic research leading to such an understanding, it is recognized that materials in their final use state (in the form of polycrystalline conglomerates) contain many imperfections. It has been shown, for example, that pure single crystal whiskers of sapphire prepared very carefully can attain a strength of as much as 1,800,000 pounds per square inch. Strengths such as this are not obtained in the engineering materials available at the present time, however, because of the presence of dislocations and defects within the crystal lattice that permit flow and fracture to occur at stress levels far below the cohesive strengths of the perfect lattice.

Materials research is, therefore, proceeding along several different lines to cope with this immediate problem. Some groups, for example, are attempting an explanation of the flow and fracture behavior of materials on an atomic level that will ultimately lead to a better understanding of the processes involved and possibly lead eventually to better engineering design concepts. Other groups are attempting empirical or semiempirical approaches, rather than exact theoretical explanations, in an effort to provide the designer with some badly needed guidance.

Research using both of these approaches is being carried on at the Lewis Research Center. Particular emphasis in the work is being placed on the environment that will be encountered in

space travel. For example, cryogenic temperatures down to that of liquid hydrogen will be encountered; corrosive media may influence fracture propagation; high-velocity meteoroid particles may transfer tremendous local energies to the material; and the type of stress field imposed may change the fracture characteristics.

FLOW AND FRACTURE CHARACTERISTICS AT THE ATOMIC LEVEL

Essential to any mechanistic study of flow and fracture in solids is the study of the properties, interactions, and motions of crystal imperfections. These are largely responsible for the departure of the mechanical properties from ideal or theoretical behavior predicted by interatomic force laws. Plastic deformation or flow is always accompanied by dislocation motion, which in turn produces point defects such as lattice vacancies, interstitials, and various agglomerates of these. These point defects along with impurities may then markedly affect the motion of dislocations and flow behavior. In order to study these phenomena, single crystals of sodium chloride and magnesium oxide were carefully prepared and tested to determine their strength characteristics (ref. 1). The experiments show that these materials possess a fair degree of inherent ductility at room temperature and that the ductility and strength are extremely dependent on the mode of specimen preparation. Also, many of the findings indicate that the nature of the surface is a prime factor in the flow behavior of the crystals. For example, the ductility of crystals of sodium chloride has been substantially increased by treatments such as surface dissolution with water, coating with a 25-angstrom layer of silver, or coating with a thin film of stearic acid. Typical results of water treatment are shown in figure 70–1. The crystals were approximately the same size and were tested in bending. Specimen A was tested in the as-cleaved condition and is shown for reference purposes. The significant point to be noted in this figure is the variation in the amount of deflection obtained prior to failure as a function of the differences in the surface treatment. (The end points of the curves signify failures.) When only the com-
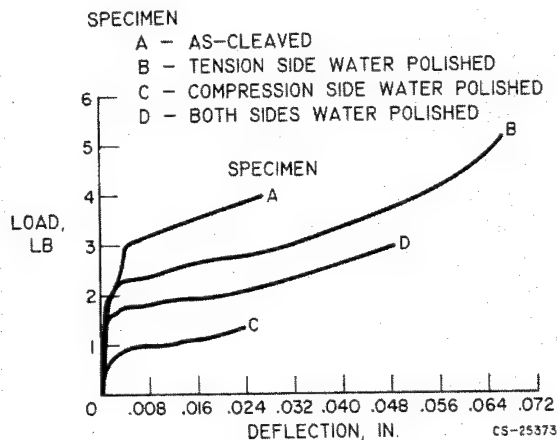

FIGURE 70–1.—Effect of surface treatment on ductility of sodium chloride single crystals.

pression side of the specimen was water polished, the ductility was roughly the same as for the as-cleaved crystal. When only the tension side was treated, however, the ductility was more than twice that of the as-cleaved crystal. The crystal polished on both sides had an intermediate ductility value. It is believed that the effect of the increased ductility obtained when the tension side was water polished is a result of the removal of surface flaws and defects. These flaws and defects provide the initiation site for the crack that ultimately propagates to produce the failure. The importance of the flaws and defects on the tension side as compared with the compression side would normally be expected. The differences in the actual load values at failure have not been satisfactorily explained.
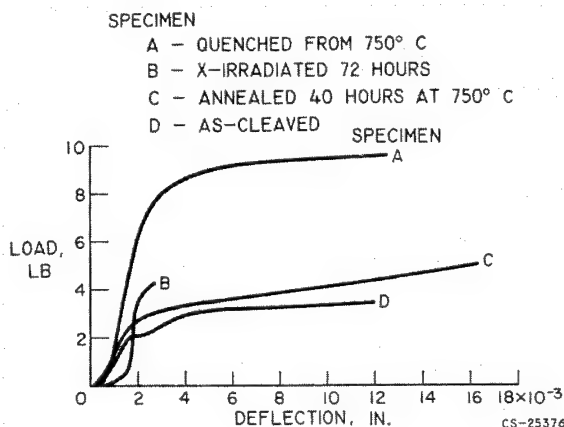

FIGURE 70–2.—Effect of bulk treatment on ductility of sodium chloride single crystals.

32

Figure 70-2 shows the effect of various bulk treatments as compared with the as-cleaved condition. These treatments are quenching from 750° C, X-irradiation for 72 hours, and annealing for 40 hours at 750° C. The point of primary interest in this figure is the very low ductility of the X-irradiated crystal compared with the other conditions, particularly the annealed condition. The irradiation effectively pins the dislocations and prevents them from moving as required for plastic flow. This phenomenon is also apparent in metals and is the subject of intense research in the consideration of materials for nuclear reactors for space vehicles. The difference in ductilities between the as-cleaved crystal of figure 70-1 and the as-cleaved crystal in figure 70-2 is indicative of the amount of scatter obtained. Despite this scatter, however, the effects of the various treatments on ductility were shown to be significant in repeated tests.

Aside from the marked changes in ductility, it is interesting to note the peculiar **S**-shape of the load-deflection curves. The initial portion of the curves, before the inflection point, is an anelastic region. In fact, at no point in the curves does the value of the slope approach the theoretical modulus for this single-crystal material. This behavior, originally thought to be unique with ionic crystals, has recently been found to occur in single crystalline metals at several other laboratories.

Although considerable progress has been made in the understanding of flow and fracture phenomena on the atomic level, the present state of the science does not permit the prediction of the performance of the polycrystalline conglomerates that must be dealt with in space engineering problems. For this reason, a number of empirical and semiempirical approaches have been proposed for predicting the strength of structures on the basis of certain parameters determined from test specimens of the material in question.

FRACTURE MECHANICS OF HIGH-STRENGTH MATERIALS

As a polycrystalline material is loaded or stressed, distortion of the crystal lattices occurs, and the bulk effect is a period during which the strain is approximately linearly proportional to the stress. As the stress increases, however, the dislocations move and produce the effect called plastic flow as the atom layers slip past each other. The imperfections or dislocations accumulate at various points within the crystal until they may be considered as voids. When a sufficient number of these voids appear, they may interconnect to produce a microscopic flaw or crack. After the appearance of these cracks, a question remains as to how much higher the material can be stressed without propagating the cracks to the point where cataclysmic failure of the structure occurs. The empirical or semiempirical approaches in general assume that the material already contains voids of a size that can be considered as cracks and would be visible to the eye if the specimen were sectioned and examined. These approaches then ignore the steps in the process prior to the formation of the cracks and attempt to predict the growth pattern of the existing cracks as the material is loaded.

One such approach is that proposed by Griffith in 1920 when he published his paper on the brittle fracture of glass (ref. 2). He postulated that the crack becomes unstable when, for a given increase in crack length, the energy decrease in the surrounding stress field exceeds the energy required to create the new crack-surface area. The suggestion was made that, for a given material, the stress σ and half the crack length a should be related as follows:

$$K = \sigma\sqrt{\pi a}$$

As the stress is increased, the constant K approaches a limiting value K_c for the given material, and the crack immediately changes from a slow growth rate to a speed near the velocity of sound in the material. The K_c parameter, therefore, is a measure of the fracture toughness of the material, and by its use the critical crack length can be calculated for a given stress. This relatively simple approach appeared to satisfy the requirements to a large degree for the completely brittle materials such as glass, but did not work well when applied to the modern high-strength alloys. Many of these alloys fail in a brittle fashion, particularly at cryogenic temperatures, and it had been hoped that the same

concept could be used. Actually, considerable plastic flow is involved at the tip of the crack, and this suggests that the crack surface energy should be augmented by the work of plastic deformation in the volume of material adjacent to the crack tip (ref. 3). Definition and measurement of this plastic work are very difficult, however. The size of the plastic zone, and, therefore, the inelastic energy it absorbs, changes with crack length and with specimen dimensions generally, as well as with the material. Measurement of the rate of energy absorption with crack growth thus requires the measurement of a variable quantity that is not a characteristic constant of material toughness.

In considerations of the stress field surrounding the crack tip, it was suggested that the plastic zone appears to the stress field as a region of somewhat relieved normal stress and is roughly comparable with an extra extension of the existing crack. This approach resulted in the following equation:

$$K_c = \sigma \sqrt{\pi \left(a + \frac{K_c^2}{2\pi\sigma_{ys}^2} \right)}$$

where the term $K_c^2/2\pi\sigma_{ys}^2$ is the required addition to the crack length to account for the plastic zone. The factor σ_{ys} is the yield strength of the material. This equation applies only to cases in which the ratio of crack length to specimen width is very small. For finite-width specimens, the equations are somewhat more complex, and a treatment of this problem is given in reference 4.

Research in the field of fracture mechanics is being carried out at the Lewis Research Center, with both uniaxial tensile specimens and biaxially stressed cylinders, as shown in figure 70–3. Cracks are simulated by machining central notches in the specimens with notch root radii as low as 0.0002 inch and determining the fracture toughness parameter K_c. The central notches are placed in the specimens by hand broaching the edges of a 0.080-inch drilled hole on a diameter of that hole perpendicular to the maximum principal stress. A photograph of these specimens is shown in figure 70–4. The test temperatures are those of primary interest in the space program because they occur in vehicle propellant tanks and life support struc-
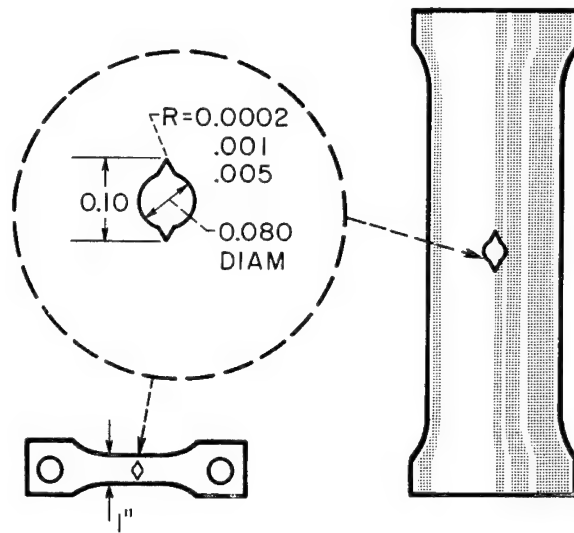

FIGURE 70–3.—Notch configuration and orientation in uniaxial and biaxial stress specimens.

tures. These temperatures range from 400° F for solid-propellant tanks to −423° F for cryogenic-propellant tanks. Considerable emphasis on the use of liquid hydrogen as a propellant in both chemical and nuclear propulsion engines centers much attention on the material properties at −423° F. The minimum weight requirements also involve the use of the highest possible strength-to-weight-ratio materials, and, in general, at −423° F the strength of notched specimens of these materials is below the yield point. Vehicle designs can not be made, therefore, on the basis of yield strength, because it must be assumed that at least one flaw or crack is probably present that escaped detection during the inspection process. This one flaw could prove disastrous if the fracture toughness of the material is not commensurate with the working stresses.

Attempts to use the uniaxial fracture toughness parameter K_c in the prediction of the fracture in the biaxial stress state of pressurized tanks have shown some signs of success, as is illustrated in figure 70–5. In this figure, the hoop burst stress for the cylinders is plotted as a function of the root radius of the notches machined in the cylinders. The material used was 2014–T6 aluminum, and the tests were conducted at two temperature levels, room temperature and −423° F. The notch radii were varied from 0.005 to 0.0002 inch. Tests re-

(a) Fractured uniaxial test specimen.

(b) Biaxial test specimen before burst.

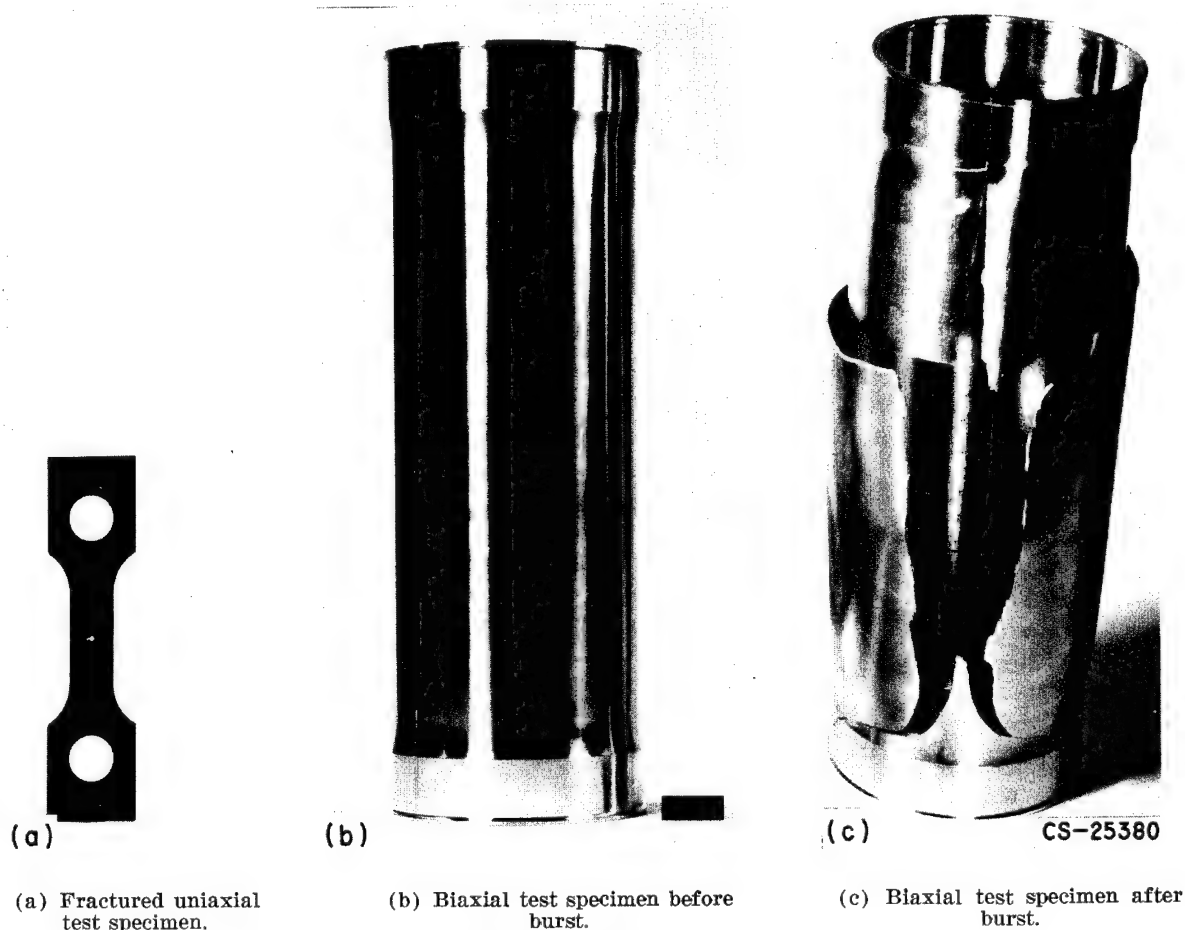(c) Biaxial test specimen after burst.

FIGURE 70–4.—Typical uniaxial and biaxial test specimens.

ported in reference 5 indicate that the 0.0002-inch-radius notch represents quite closely the performance of specimens having an actual crack. The data for less sharp notches were obtained to determine their effect on the cylinder strengths. The solid lines represent the predicted strength of the cylinders based on K_c values determined from tensile specimens having the same type of notches. In addition, it was necessary to make a correction to the size of the plastic zone at the tip of the crack in the cylinders in order to get the good agreement shown in figure 70–5. At −423° F it was necessary to reduce the plastic zone size correction to a value of 46 percent of that required for uniaxial tensile specimens. At room temperature, the required reduction was 68 percent.

Figure 70–5 also shows the computed hoop stress where yielding would occur in the cylinders based on the equivalent stress being equal to the uniaxial yield stress. For a notch root radius of 0.0002 inch, the failure stress of the cylinders was approximately 80 percent of the computed yield strength for both room temper-
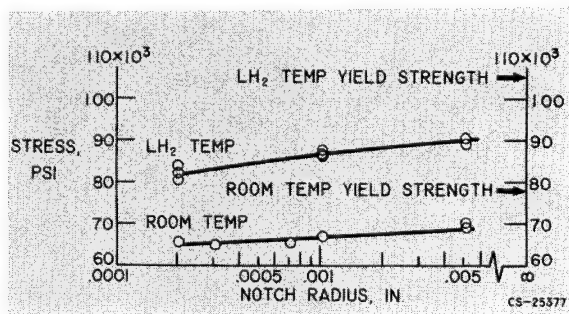

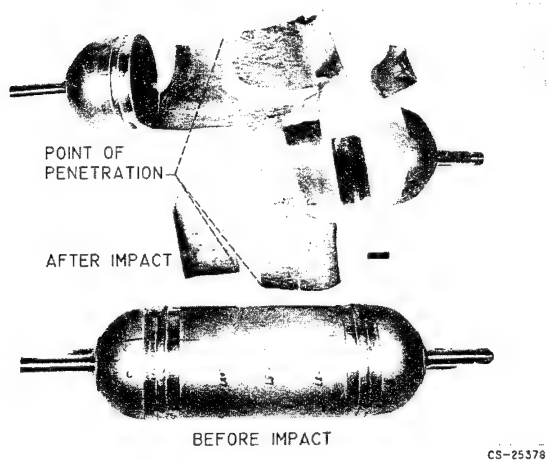FIGURE 70–5.—Correlation of burst strength of notched 2014–T6 cylinders with modified Griffith-Irwin theory.

FIGURE 70-6.—Effect of high-speed particle impact on 2014–T6 aluminum tank filled with water.

ature and liquid-hydrogen temperature, which illustrates the danger of basing the design on yield strength for the case where there can be a small defect and the material shows a notch sensitivity.

FLOW AND FRACTURE ASSOCIATED WITH HYPERVELOCITY IMPACT

Another interesting facet of the problem of flow and fracture of the high-strength materials used for propellant tanks lies in the area of hypervelocity impact. This problem is, of course, associated with the impact of meteoroids with space vehicles. These particles can be traveling at velocities from about 36,000 to 200,000 feet per second relative to the spacecraft.
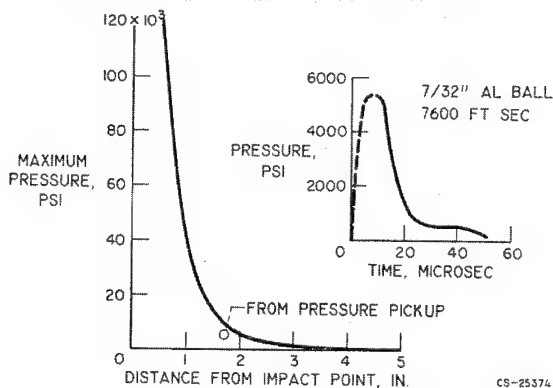
FIGURE 70-7.—Pressure generated in water-filled tank by high-speed particle impact.

If there is no liquid in contact with the wall that is impacted, the worst that will result is probably a clean hole that has some possibility of being patched or self-sealed in some fashion. If a liquid is in contact with the impacted tank wall, shock waves will be created in the liquid and will produce very high pressure forces. Figure 70-6 shows the results of firing a small aluminum pellet at about 7000 feet per second into a pressurized tank containing water. Similar experiments in which only a pressurized gas was contained in the tank resulted in a simple hole without the catastrophic damage illustrated.

An example of the pressures generated in the contained liquid at impact is illustrated in figure 70-7. These pressures were measured by means of high-speed photographs of shock waves traveling in water away from the point of impact. It can be seen that pressures well in excess of 100,000 pounds per square inch can be generated. These pressures are localized and result in a local initial failure, but the stored energy from pressurization within the tank can result in complete tank failure. Such a failure would immediately terminate the mission of a space vehicle and must be avoided at all costs.

The pressure pulse causing the failure is of short duration, as illustrated in the inset of figure 70-7. The pressure rapidly decays a few inches away from the point of impact. In order to be sure that the failure was occurring as a result of this initial high-pressure pulse, and not from a reflected shock wave, high-speed photographs were taken of the failure. A picture sequence of the failure is shown in figure 70-8. It can be noted that the first crack radiating from the point of impact was visible only 28 microseconds after impact. During the first 28 microseconds the shock wave in the water had a chance to travel less than 2 inches from the point of impact, and the shock wave in the metal only $5\frac{1}{2}$ inches. It is thus clearly illustrated that the initial failure mechanism was local in nature.

The results shown were for tanks containing water. From analytical studies, the compressibility of the liquid is believed to have a significant effect on the impacting energy required to cause catastrophic failure. In addition, the
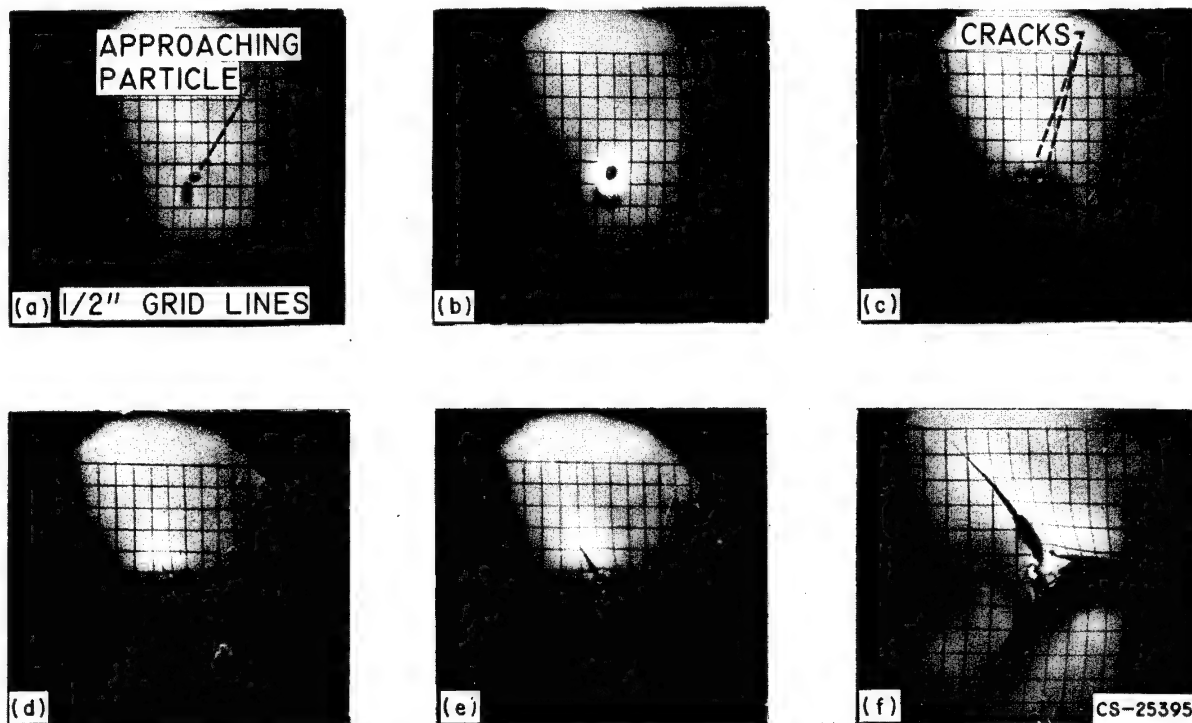
(a) Before impact.
(b) Impact.
(c) At 28 microseconds.
(d) At 50 microseconds.
(e) At 83 microseconds.
(f) At 210 microseconds.

FIGURE 70–8.—Crack propagation as a result of high-speed particle impact on water-filled tank. Impacting particle, 7/32-inch-diameter aluminum sphere; particle velocity, 5780 feet per second.

temperature of the fluid will be important because of its effect on the material properties of the tank wall. Cryogenic propellants will make the walls more susceptible to brittle fracture. Liquid oxygen, because of lower compressibility, may present more of a problem than liquid hydrogen. Future research programs will concentrate on studying the failure mechanism with these liquids.

As a matter of general interest, some preliminary results have also been obtained on reactions that occur when high-speed impacts occur on tanks containing liquid oxygen. For tanks made of aluminum or stainless steel containing liquid oxygen, impacts at velocities up to about 7500 feet per second resulted in rupture of the tanks, but there was no burning of the tank material due to the presence of liquid oxygen. When the tank wall was made of titanium alloy (5 percent aluminum, 2½ percent tin), a very violent reaction occurred. After impact, a series of detonations occurred, and the subsequent burning consumed the titanium wall. A photograph of the impact in figure 70–9, taken from a single frame of a 16-milli-meter movie, shows one of the detonations that occurred. It is obvious, therefore, that, even though titanium may have weight advantages for use in lightweight propellant tanks, there is a question as to whether to use it in oxidant tanks because of its high reactivity.

SUMMARY

The problem of flow and fracture in high-strength space vehicle materials has been shown to be very complex. It was indicated in particular how the problem can be influenced by environmental factors such as cryogenic temperatures and extremely high impact velocities of meteoroids. Investigations range from the atomic to the macroscopic level. It is hoped that eventually, when sufficient knowledge has been acquired, it will be possible to merge the seemingly divergent approaches now be-
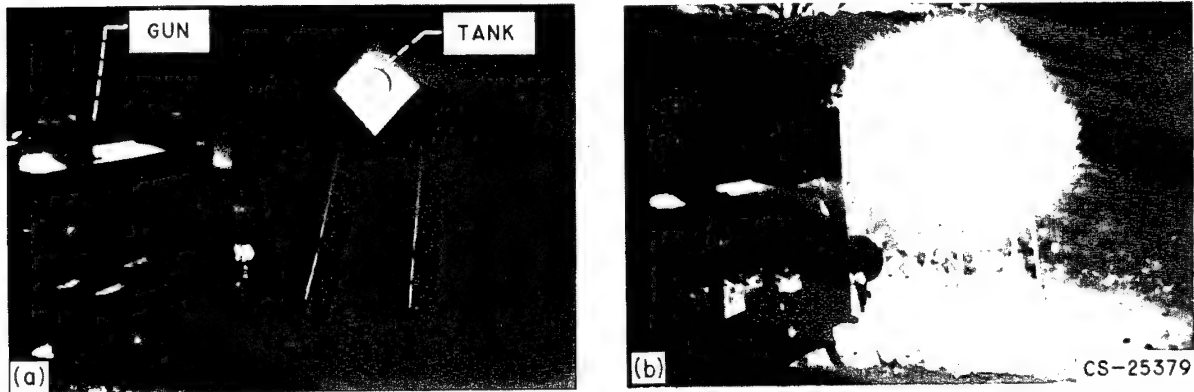
FIGURE 70–9.—Effect of impact of high-speed particle on titanium tank containing liquid oxygen.

ing used into one basic concept that will enable the designer of a vehicle to arrive at a satisfactory design with an exceedingly high degree of reliability. It is obvious that much additional research is, therefore, required to attain this goal.

REFERENCES

1. STEARNS, CARL A., PACK, ANN E., and LAD, ROBERT A.: Ductile Ceramics. I—Factors Affecting the Plasticity of Sodium Chloride, Lithium Fluoride, and Magnesium Oxide Single Crystals. NASA TN D–75, 1959.
2. GRIFFITH, A. A.: The Phenomena of Rupture and Flow in Solids. Phil. Trans. Roy. Soc. (London), ser. A, vol. 221, Mar. 1921, pp. 163–198.
3. IRWIN, G. R.: Fracture Dynamics. Fracturing of Metals, ASM, 1948.
4. First Report of a Special ASTM Committee: Fracture Testing of High-Strength Sheet Materials. ASTM Bull., Feb. 1960.
5. Third Report of a Special ASTM Committee: Fracture Testing of High-Strength Sheet Materials. Materials Res. Standards, vol. 1, no. 11, Nov. 1961.

High-Strength Materials Research

By Hubert B. Probst

DR. HUBERT B. PROBST, *who is currently working on the properties of high-temperature nonmetallics, is Head of the Refractory Compounds Section of the NASA Lewis Research Center. He earned his B.S. in Metallurgy from the University of Notre Dame in 1953, his M.S. from the University of Michigan in 1954, and his Ph. D. from Case Institute of Technology in 1959. Dr. Probst is a member of the American Society for Metals and Sigma Xi.*

The need for high-strength materials in aircraft and space applications stems from two necessities. First is that of weight savings; a high-strength material is able to sustain a given stress with a minimal cross section. Second is the need to combat the loss of strength that generally accompanies increased temperatures; many applications, particularly in powerplants, require stressed members to operate at high temperatures—thus the need for retention of strength to high use temperatures.

Some of the research that is in progress at the Lewis Research Center and that is devoted to improved strength characteristics of materials is reviewed herein. The review is made according to temperature ranges and covers many areas of vastly different materials and applications. The common thread in all these programs is improved strength.

When it is considered that the cost to orbit 1 pound of material about the Earth is in excess of $1,000, the savings attendant to weight reductions by the use of high-strength materials is evident.

Figure 71–1 (ref. 1) compares a number of materials on a basis of strength-to-density ratio. The more conventional materials such as steels, titanium alloys, and aluminum alloys offer ratios of the order of 1 to 2 million. Beryllium shows some improvement over these. The fiber materials give the next step in improved strength-to-density ratios; however, they are

directional and must be oriented in the direction of the principal stresses and must be held together by a binder. Glass-reinforced plastics are present-day examples that utilize fiber strengths. In the field of propellant tanks, an attempt has been made to capitalize on the strength of a directional material by filament winding. The extremely strong whisker materials with ratios in the 12 to 24 million range hold promise for the future; however, there is much progress yet to be made toward quantity production and fabrication. The subject of whiskers is discussed later. Although alloys do not offer ultra high strength-to-density ratios, they are the materials in use today, and their shortcomings must be considered.

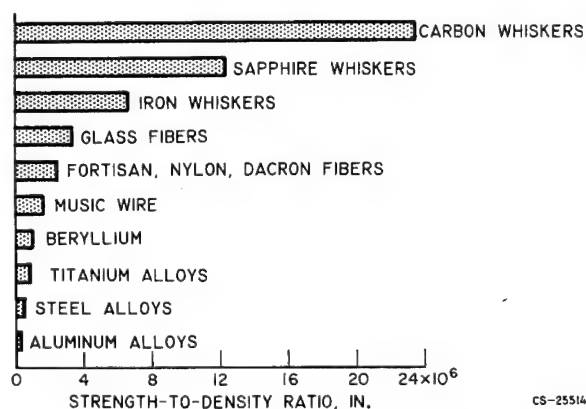Consider first the room-temperature strength

FIGURE 71–1.—Material strength-to-density ratios.

characteristics of alloys. An example of a quite serious problem in this temperature range is given in figure 71–2, which shows a solid-pro-
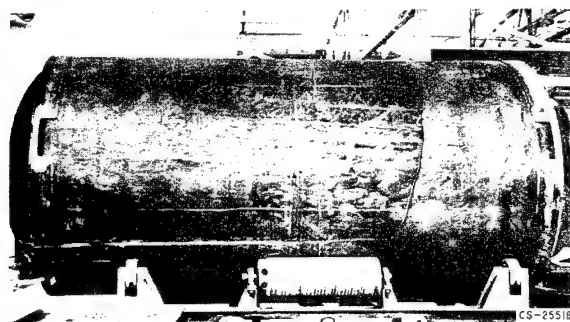

FIGURE 71–2.—Brittle fracture of large rocket motor case.

pellant motor case that failed during room-temperature pressure testing (photograph obtained from W. F. Brown, Jr. of Lewis). The failure is catastrophic and occurred at a stress level of only about 50 percent of the normal yield strength. Such a failure is attributed to the presence of small yet highly damaging cracks usually in the areas of welds. Such a crack can propagate unstably through otherwise sound material resulting in the catastrophic failure shown. Further insight into this problem is gained from figure 71–3 (ref. 2) in which the conventional tensile strength of smooth bar specimens is plotted against tempering temperature for a steel similar to that used in the rocket motor case. The material was heat treated in the 800° to 900° F range to give maximum tensile strength; however, a determination of strength for sharp-notched specimens gave the
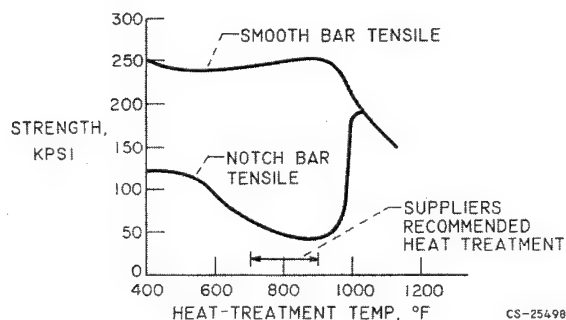
lower curve. It is apparent that the recommended tempering temperature has resulted in a minimum in notch strength, which accounts for the failure that occurred at a stress level far below the conventional tensile strength. This situation has, of course, been greatly improved by altering the heat treatment to one that results in higher notch strengths.

With this room-temperature behavior in mind, consider the effect of lowering temperature to the cryogenic range. In this range, the main concern for high-strength materials is for rocket cases and propellant tanks. Since these components represent a large portion of the total vehicle weight, significant weight reductions are possible by the use of thinner walls of higher-strength material. It is generally true that lower temperature results in increased strength, so that a lessening of problems stemming from material-strength considerations might be anticipated as lower temperatures are approached. Specifically, an improvement in the situation in progressing from present-day vehicles using liquid oxygen at $-297°$ F to future systems requiring liquid hydrogen at $-423°$ F is desired. Figure 71–4 (ref. 3) compares data for AISI–301 stainless steel and an alpha titanium alloy and shows the anticipated gains in strength; however, the problems are by no means lessened, because the presence of defects again is of major concern. This is illustrated in the curves plotted for sharp-notch strengths, which decrease below a certain tem-
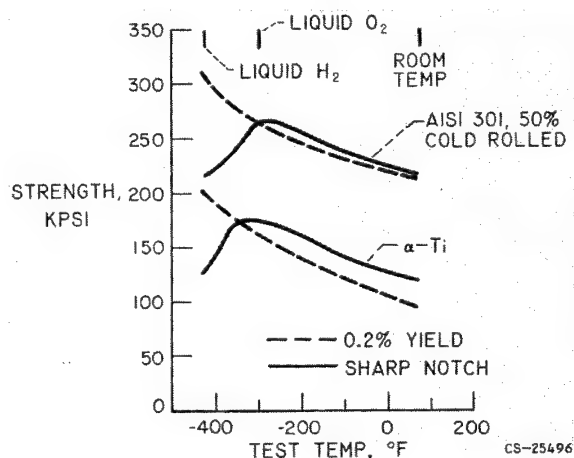

FIGURE 71–3.—Comparison of strength of smooth and notched specimens of steel at room temperature.

FIGURE 71–4.—Effect of cracks on strength of alloys tested at various temperatures.

perature. This increased sensitivity to the embrittling effects of notches renders the material vulnerable to catastrophic failure, as already illustrated in the failure of the motor case at room temperature.

Since the tanks of space vehicles will be large structures in which detection or elimination of all flaws introduced during the various fabrication processes is impossible, the behavior of materials with flaws or notches at cryogenic temperatures becomes of utmost importance to the designer. Along these lines, work at the Lewis Research Center is continuing in the development of testing methods to evaluate resistance to catastrophic failure and formulation of suitable criteria for rating materials for thin-walled cryogenic-pressure-vessel service. Significant contributions have already been made in this area. With these newly developed test methods, such variables as heat treatment, composition, and melting and fabrication practices are being investigated.

At elevated temperatures, the need for high-strength materials arises from the weight-savings consideration but primarily from the desire to increase operating temperatures of powerplants. The maximum operating temperature of a powerplant is usually set by the materials available. Thus, the quest for superior material is made to allow operating temperatures to increase.

One effective means of strengthening a metal or an alloy is to disperse fine particles throughout the matrix which serve to inhibit dislocation glide (slip) and creep and generally allow for higher strengths at higher temperatures. This effect was observed in 1919 (ref. 4) in the age hardening of an aluminum alloy and is attributed to a precipitation reaction. About 15 years ago, strengthening of extruded aluminum powder was observed (ref. 5) and attributed to thin oxide layers (aluminum oxide), which were broken into fine particles during the extrusion process and inhibited flow of the aluminum. This material, generally referred to as SAP (sintered aluminum powder), gave considerably improved strengths and use temperatures to aluminum, as shown in figure 71–5 (ref. 6). The higher use temperature of SAP is a result of the fact that it is a nonequilibrium structure.
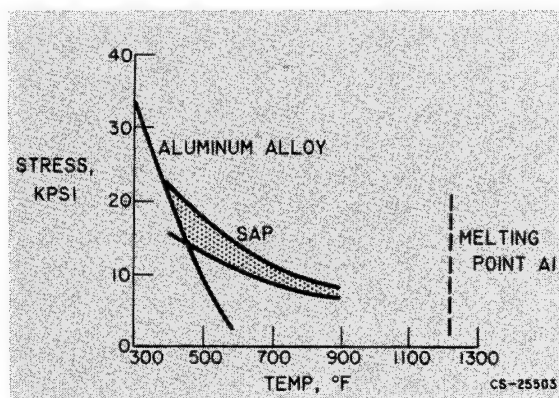

FIGURE 71–5.—Stress-temperature curves for rupture in 1000 hours (ref. 6).

Compared with an equilibrium structure, such as a precipitation-hardened aluminum alloy whose strength is lost at elevated temperatures because of complete dissolution of the strengthening precipitate, the oxide particles in SAP remain stable at such temperatures and continue to strengthen. Since the introduction of SAP, great effort has been put forth to apply such principles to higher melting metals in the hope of increasing use temperatures.

The oxide particles in SAP are spaced approximately 0.3 micron apart, and it is felt that such a submicron spacing is necessary to achieve the full potential strengthening benefits of the dispersed particles. Of the several methods by which fine dispersions may be produced, the approach taken at Lewis has been to mix directly powders of dispersant and matrix. This, of course, requires powders of submicron size. The production of such metal powders by normal attrition methods is difficult because of particle agglomeration that occurs before the submicron range is reached. Submicron powders have resulted from a study at Lewis (ref. 7) in which various grinding aids were used to prevent agglomeration. It is believed that such aids prevent agglomeration by reducing electrostatic attraction and by reducing the tendency of the particles to weld together. The effect of one such aid, potassium ferricyanide ($K_3Fe(CN)_6$), is shown in figure 71–6 (ref. 7). For a number of metal powders with starting sizes as large as 30 microns, final particle sizes less than 1 micron have been achieved in conventional ball mills.

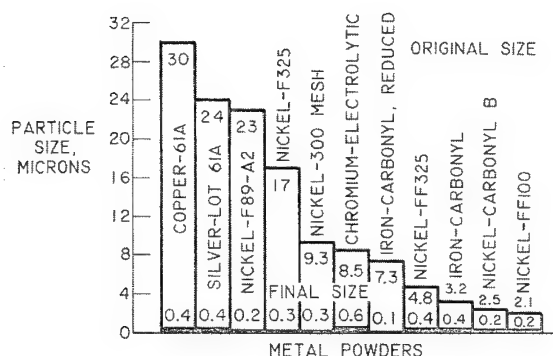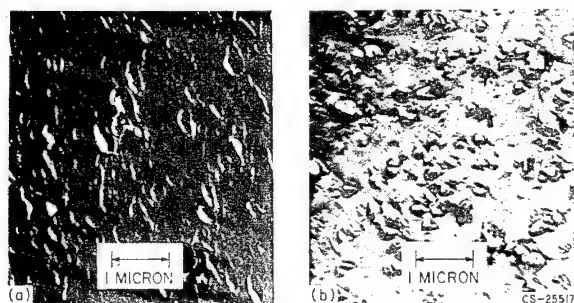With such powders, structures quite similar to

FIGURE 71–6.—Use of potassium ferricyanide to grind various metal powders. Milled for 15 days in 200-proof ethyl alcohol.

(a) Aluminum oxide in nickel.
(b) SAP.

FIGURE 71–7.—Comparison of microstructures of aluminum oxide dispersed in nickel and SAP. ×20,000.
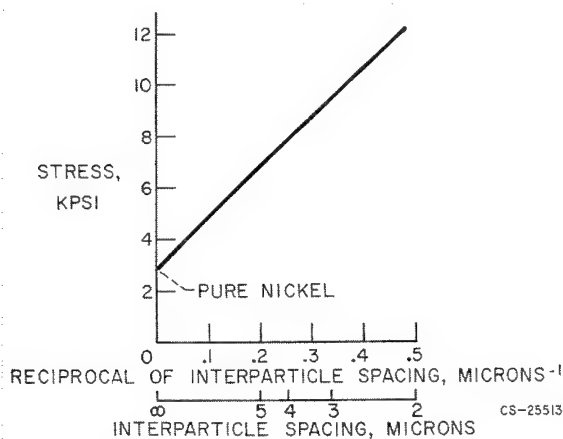

FIGURE 71–8.—Stress to cause rupture in 10 hours at 1500° F against reciprocal of measured interparticle spacing for nickel-aluminum oxide system (ref. 8).

those of SAP have been produced as shown in figure 71–7 (unpublished data of J. W. Weeton of Lewis). Here, finely dispersed aluminum oxide in nickel is compared with a typical SAP structure. The $Ni-Al_2O_3$ structure was prepared by direct mixing of the two powders followed by extrusion. With such materials, the basic effects of particle sizes and interparticle spacing are now being studied in a variety of systems. Past results with the $Ni-Al_2O_3$ system show a strong effect of particle spacing on strength as shown in figure 71–8 (ref. 8). The stress required to cause failure in 10 hours at 1500° F is shown to vary directly as the reciprocal of the interparticle spacing. Also, note the strengthening over pure nickel.

Another means of attaining improved strength is the conventional alloying approach. In this method an attempt is made to strengthen existing phases and produce new phases that will contribute to strength; these effects are brought about by judicious control of composition. Such a program has been in progress at the Lewis Research Center for several years (refs. 9, 10, and 11). The basic composition in weight percent of the experimental alloy is as follows:

Mo	Cr	Al	Zr	Ni
8	6	6	1	Bal.

The major additions to the basic alloy were
  Carbon
  Titanium
  Titanium plus carbon
  Vanadium plus carbon
  Tungsten plus vanadium plus carbon
  Tantalum plus tungsten plus vanadium
    plus carbon
Chromium and aluminum have been added primarily for oxidation resistance and molybdenum for solid-solution strengthening. Zirconium is believed to stabilize the composition against diffusion losses (ref. 12). Modifications to the base composition were made in attempts to get dispersed phases and strengthening.

The resulting strengthening is shown in figure 71–9 (ref. 11). The more complex tantalum-tungsten-vanadium-carbon modification has led to the greatest improvement. Increased stress-rupture lives are dramatic at 1800° F, for example. Also of importance is the improve-
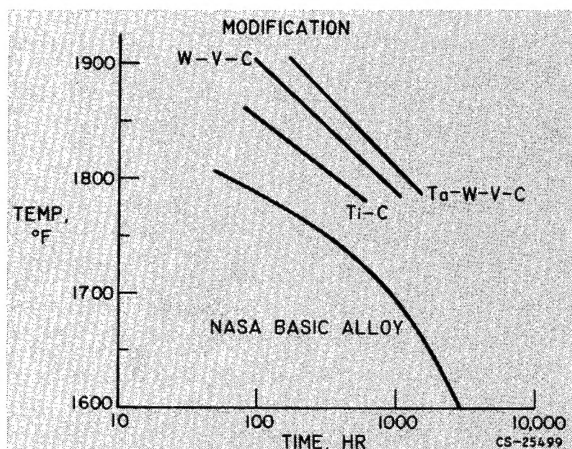
FIGURE 71–9.—Stress-rupture comparison at 15,000 psi stress of nickel-base alloy series.

ment in use temperature; for example, for a 200-hour life at 15,000 psi, the use temperature has been increased from 1760° to 1900° F.

Admittedly, with such complex compositions, it is difficult to define a singular strengthening mechanism; however, in the case of the Ta-W-V-C modification, electron diffraction has identified the Ni_3Al intermetallic and the carbides TaC and MoC. The presence of a nickel-aluminum-vanadium intermetallic and complex carbides is also suspected.

Of major importance to such highly alloyed compositions is workability, that is, the avoidance of complete embrittlement by the strengthening additions. The workability of the Ta-W-V-C-modification is illustrated in figure 71–10. The upper portion of the figure shows cross sections of a ¾-inch cylinder before and after forging at room temperature. The lower portion shows cross sections after various reductions. No cracking occurred, and no intermediate stress relief anneals were used. The maximum reduction in diameter is 29 percent; however, with the use of intermediate anneals, diameter reductions as high as 50 percent can now be obtained.

Work with this basic alloy is continuing both at Lewis and in industry. At Lewis, new efforts are under way to apply similar principles to cobalt-base alloys.

A dramatic approach to high-strength materials is to capitalize on the high strengths of fibers and whiskers. Figure 71–11 (ref. 13)
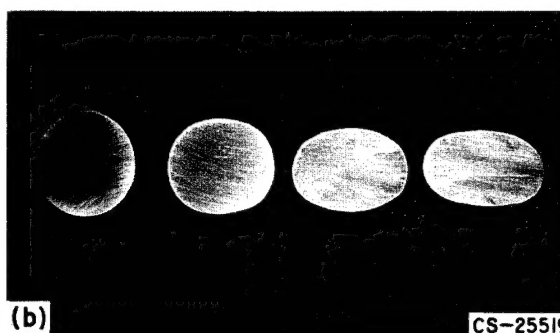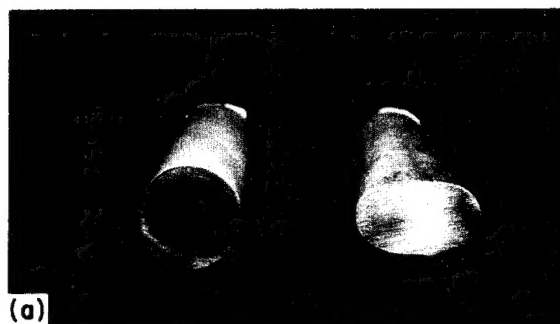

FIGURE 71–10.—Deformation of cold-forged bars of strongest tantalum-modified alloy.

shows the relation between strength and material size. This effect is believed to be a result of the attainment of more perfect structures at smaller sizes with extreme strengths being reached at the dimensions of whiskers of 1 to 10 microns, which have been shown to contain very few defects; in some cases, only one screw dislocation.

Past efforts at Lewis have sought to make practical use of the high strength of tungsten fibers by embedding them in a copper matrix.
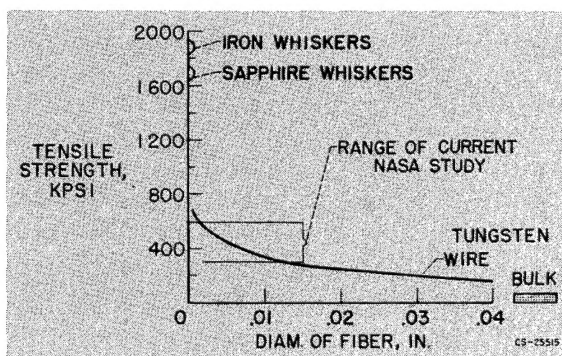

FIGURE 71–11.—Strength of whiskers and fibers at room temperature.
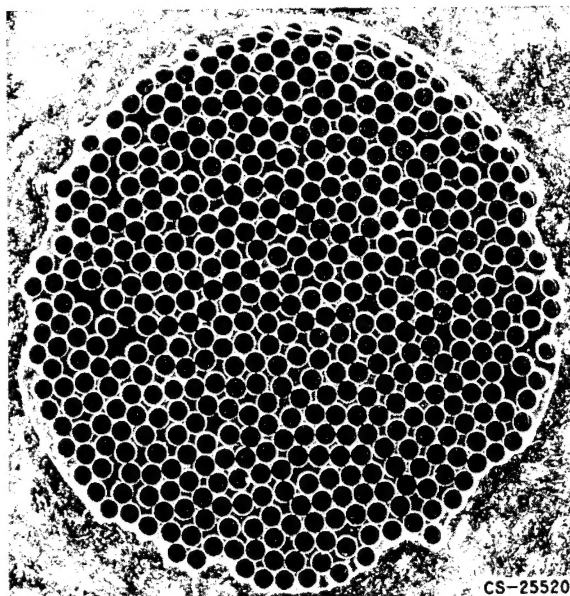
FIGURE 71-12.—Transverse section of tungsten-reinforced-copper composite; 483 wires of 5-mil diameter. ×50.

This is done by infiltrating liquid copper into a bundle of tungsten wires, resulting in the structure shown in figure 71-12 (ref. 13). Such composites have been prepared at various wire-to-matrix volume ratios and strengths measured.

Figure 71-13 (ref. 13) shows some of the results. The strengths of bulk copper and tungsten fiber are shown along with two composite compositions. The strength of the composite increases directly with the number of fibers present. These data are for composites containing continuous tungsten fibers; that is, the fibers run the entire length of the tensile speci-
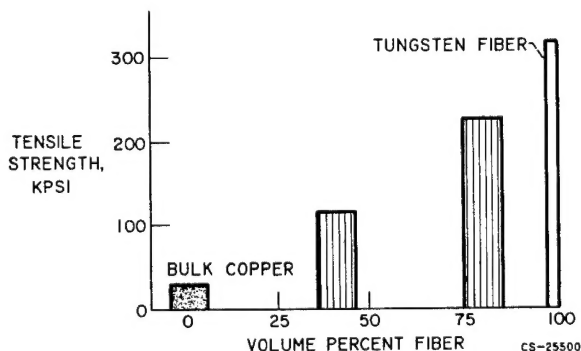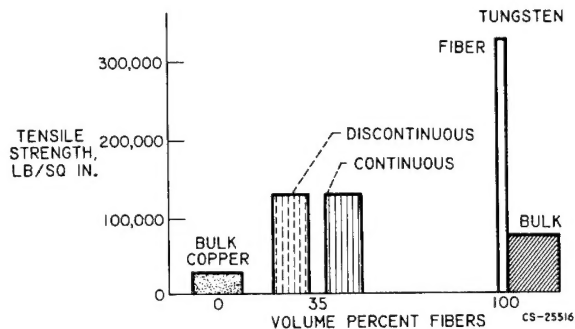

FIGURE 71-14.—Tensile strength of tungsten-copper composite with continuous and discontinuous tungsten fibers.

men. This brings up the immediate question, Would the tungsten fibers contribute to the composite strength if they were not continuous? This question has been answered by preparing composites in which the tungsten fibers were present as short discontinuous lengths. Some of the results are shown in figure 71-14 (ref. 13). This partciular figure for 35 volume percent fiber shows the discontinuous fiber to be just as effective in strengthening as the continuous fiber. The strength of bulk tungsten is also shown for comparison.

The fact having been established that discontinuous fibers are effective strengtheners, the possibility of replacing wire and fibers with short lengths of whiskers becomes intriguing. This would make possible the achievement of ultra high strengths approaching those of whiskers in useful bodies of reasonable size.

Work in this field is continuing at Lewis. A complete understanding of the mechanism by which discontinuous fibers contribute to strengthening is being sought along with a description and understanding of the elastic and plastic behavior of such composites. Copper, iron, and alumina whiskers are also being produced and used in studies of true whisker composites.

At higher temperatures, those beyond the range of the nickel or cobalt superalloys, refractory metals (W, Mo, Cb, Ta) become of interest. Figure 71-15 (refs. 14 and 15) shows high-temperature–strength curves for molybdenum, two commercial molybdenum alloys, and tungsten. Tungsten is superior at all temperatures and retains useful strength even at 4400° F.
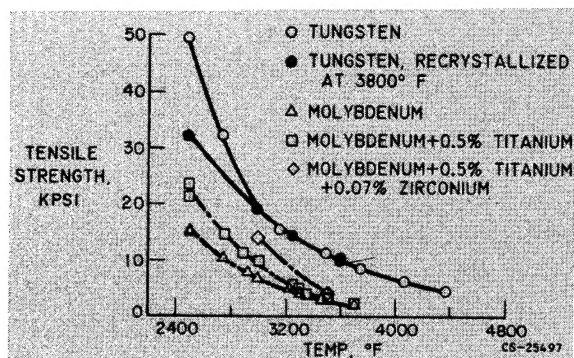

FIGURE 71-13.—Tensile strength of tungsten-copper composites with continuous tungsten fibers.

FIGURE 71-15.—Tensile strength of tungsten, molybdenum, and molybdenum alloys at high temperatures.

FIGURE 71-16.—High-temperature tensile strengths of tungsten-base alloys.

Since tungsten has the highest melting point of all metals (6170° F) and appears to offer the most potential for higher use temperatures, the major portion of the refractory metals program at Lewis is devoted to tungsten. Tungsten-alloy compositions of improved strength are being sought by both powder-metallurgy and arc-melting techniques. Strengths of some of the better alloys produced to date are shown in figure 71-16 (from unpublished data of P. Raffo of Lewis). These data are for arc-melted alloys after extrusion. The improvements offered by these binary compositions are encouraging. It is thought that the tantalum and columbium additions are resulting in solid-solution strengthening, while the boron addition gives grain refinement, which contributes to strengthening. More recent results predict that still further improvements can be expected by ternary and more complex compositions.

Tungsten as well as other body-centered cubic metals exhibits a transition temperature, that is, a temperature below which the metal behaves in a brittle manner and above which it possesses plasticity and exhibits some ductility before fracture. The transition temperature of tungsten in structural sizes is usually in the range of 200° to 500° F, which, of course, places room temperature, where tungsten parts must be handled, in the brittle range. Research into this transition behavior and attempts to lower the transition temperature are therefore of extreme importance. The transition behavior, as well as strength characteristics, has long been thought to be associated with and controlled by interstitial impurities, primarily carbon and
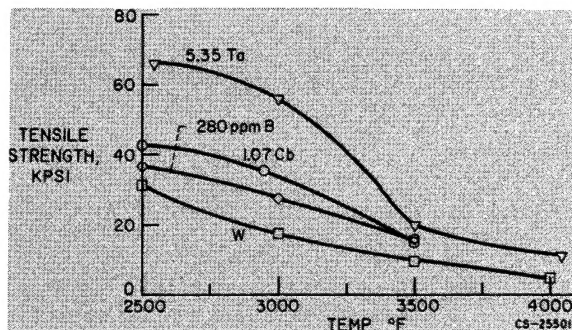
oxygen. In recent work at Lewis (ref. 16) in which controlled amounts of these impurities were introduced separately into high-purity polycrystalline and single-crystal tungsten, the role of each impurity has been elucidated. The results are too involved to cover here; however, they do show different effects of the two interstitials studied. The effect of carbon is believed to be one restricted to the lattice, possibly a Cottrell dislocation-locking mechanism, while the effect of oxygen appears to be isolated to high-angle grain boundaries.

For certain high-temperature applications beyond the range of refractory metals, the so-called hard metals or interstitial compounds are of interest. As part of this group, the refractory carbides are of particular interest since they represent the highest melting materials known. For example, hafnium carbide and tantalum carbide are the highest melting simple carbides with melting temperatures of approximately 7000° F.

Such materials are consolidated by powder-metallurgy techniques and are subject to some degree of porosity. Strengths of these materials are related to porosity and grain size. A determination of how each of these factors effects the strength of hafnium carbide and, consequently, the development of optimum combinations for maximum strength, are the goals of a current project at Lewis.

In summary, some of the research at the Lewis Research Center devoted to high-strength materials has been reviewed. A great variety of materials with use temperatures ranging from −423° to over 5000° F are being studied, and it is hoped that the reader's interest has been stimulated in some of these areas.

REFERENCES

1. ESGAR, JACK B.: Cryogenic Propellant Tank Structures. Aviation Conf., ASME (Wash., D.C.), June 26–28, 1962.
2. ESPEY, G. B., JONES, M. H., and BROWN, W. F., JR.: A Preliminary Report on Sharp Notch and Smooth Tensile Characteristics for a Number of Ultra High Strength Sheet Alloys. Proc. ASTM, vol. 59, 1959, pp. 837–871.
3. ESPEY, G. B., JONES, M. H., and BROWN, W. F., JR.: Factors Influencing Fracture Toughness of Sheet Alloys for Use in Lightweight Cryogenic Tankage. Symposium on Evaluation of Metallic Materials in Design for Low-Temperature Service, Spec. Tech. Pub. 302, ASTM, 1961.
4. MERICA, P. D., WALTENBERG, R. C., and SCOTT, H.: Heat Treatment of Duralumin. Bull. AIME, 150, 1919, pp. 913–949.
5. IRMANN, R.: Sintered Aluminum with High Strength at Elevated Temperatures. Metallurgia, vol. 46, no. 275, Sept. 1952, pp. 125–132.
6. CROSS, H. C., and SIMONS, W. F.: Alloys and Their Properties for Elevated Temperature Service. Utilization of Heat Resistance Alloys, ASM, 1954.
7. QUATINETZ, MAX, SCHAFER, ROBERT J., and SMEAL, CHARLES: The Production of Submicron Metal Powders by Ball-Milling with Grinding Aids. Trans. AIME, vol. 221, Dec. 1961.
8. CREMENS, W. S., and GRANT, N.J.: Preparation and High Temperature Properties of Nickel–Al_2O_3 Alloys. Proc. ASTM, vol. 58, 1958, p. 714.
9. FRECHE, JOHN C., RILEY, THOMAS J., and WATERS, WILLIAM J.: Continued Study of Advanced-Temperature Nickel-Base Alloys to Investigate Vanadium Additives. NASA TN D–260, 1960.
10. FRECHE, JOHN C., WATERS, WILLIAM J., and RILEY, THOMAS J.: A New Series of Nickel Base Alloys for Advanced-Temperature Applications. Trans. ASM, Spring, 1961.
11. FRECHE, JOHN C., WATERS, WILLIAM J., and RILEY, THOMAS J.: A New Series of Advanced-Temperature Nickel-Base Alloys. High Temperature Materials Symposium, AIME, Cleveland (Ohio), Apr. 1961.
12. DECKER, ROWE, and FREEMAN: Physical Metallurgy of Nickel-Base Super-alloys. DMIC Rep. 153, May 5, 1961.
13. McDANELS, D. L., JECH, R. W., and WEETON, J. W.: Metals Reinforced with Fibers. Metals Progress, December 1960.
14. HALL, ROBERT W., and SIKORA, PAUL F.: Tensile Properties of Molybdenum and Tungsten from 2500° to 3700° F. NASA Memo 3–9–59E, 1959.
15. SIKORA, PAUL F., and HALL, ROBERT W.: High-Temperature Tensile Properties of Wrought Sintered Tungsten. NASA TN D–79, 1959.
16. STEPHENS, J. R.: Effects of Interstitial Impurities on the Ductility of Tungsten. Paper Presented at AIME Meeting, New York (N.Y.), Oct. 1962.